HÖGSKOLAN I BORÅS

INSTITUTIONEN INGENJÖRSHÖGSKOLAN

THE METHOD OF MOMENT FOR THE ELECTROMAGNETIC SCATTERING FROM BODIES OF REVOLUTION

Muath Gouda

FINAL DEGREE THESIS 30 ECTS, THESIS NO.: 4/2008
M.Sc. Electrical Engineering - Communication & Signal Processing

The Method of Moment for the Electromagnetic Scattering from Bodies of Revolution

Muath Gouda
E-mail: muath.gouda@gmail.com

Final Master's Degree Thesis
Subject Category: Electrical Engineering
Series Number: 4/ 2008

University College of Borås
School of Engineering
SE-501 90 Borås
Telephone: +46 33 435 46 40

Examiner: Dr. Samir Al-Mulla
Supervisor: Dr. Samir Al-Mulla
E-mail: samir.al-mulla@hb.se
Client: Högskolan i Borås
Date: 20th of October, 2008

ABSTRACT

The scattering problem for electromagnetic waves by perfect conducting bodies of revolution is very important for many researchers. The Method of Moment (MoM) has been used for solving the problem of scattering by a three dimensional body of revolution. The radiation boundary condition applied to truncate the partial differential equation (PDE) mesh, is based upon an asymptotic expansion derived by Wilcox. Numerical results illustrating the procedure and verifying the accuracy of the results are included. These results are compared with other calculations.

Acknowledgements

I wish to convey my deepest gratitude and cordial thanks to my supervisor Dr. Samir Almulla, for his valuable suggestions, beneficial advice and moral support throughout this work.

I feel extremely indebted to Dr. Yousef Khazmi for his unlimited help and moral support in Mathematica program. Without his beneficial encouragement, help and advices this work would never have been what it is now.

I would like to express my special thanks and appreciation to my wife Sarah, without her support this thesis would not have been possible.

I would also like to express sincere thanks to my group mate Muhammed Aamir Latif for hard work and many long hours of coordination.

Last but not least, I would like to send my grateful thanks to all the staff members in the Communication and Signal Processing Department and all those who helped me to accomplish this work.

INDEX:

CHAPTER ONE

INTRODUCTION

1.1 Introduction:

A large number of structures in the field of electromagnetic have been a huge field of researches in the last thirty years. There are structures that have rotational symmetry, on to which it is desirable to mount certain electromagnetic device, for example, the fuselage of an aircraft or missile. Since the electromagnetic is the scientific discipline that deals with electric and magnetic sources and the field of these sources produce in specified environment, the periodic behavior of the electromagnetic fields around this type of structure is known, and it is possible to extract this behavior analytically by starting from the start point in these types of problems which is the Maxwell's equations with some addition of certain principles and theorems. Figure (1.1) shows the general electromagnetic transfer function.

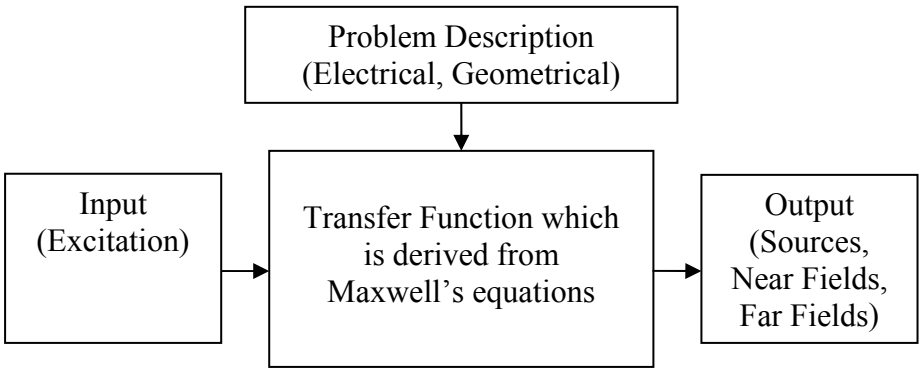

Fig (1.1): Electromagnetic Transfer Function [1]

A general electromagnetic can be defined as: when electromagnetic waves are incident on a scattered, it produces currents in the surface. These currents radiate and produce the scattered field. Now, the problems can be either solved in frequency domain or time domain by constructing integral equations for the current that is on the surface of the body. These currents are determined and from these surface current, the scattering field can be computed directly.

When we come to the term associated with the scattering problems, the Radar Cross Section (RCS) comes up. To calculate the RCS, we can consider three basic lines to calculate it; they are prediction, reduction and measurement. For the prediction part, there are two methods that are used to predicate the RCS and they are analytical method and numerical method.

The analytical methods are available in the time domain or frequency domain when the target is coincides with the coordinate systems (rectangular, spherical and cylindrical). This method is separation of variables [2-3].

The other methods, numerical methods, are developed to solve RCS for the complex targets. This method depends also in the usage of the time domain or frequency domain, scattering regimes and target geometry.

In the coming part, some theories for RCS prediction techniques are presented. From these theories, we can find the advantage and disadvantage of these techniques.

- **Geometrical Optics (GO):**

This theory is based on three concepts:
- Rays are reflected in mirror fashion from the surface.
- Rays that pass through the surface from one medium into another are reflected.
- Energy flows in a direction perpendicular to surface of constant phase.

The Geometrical Optics theory has several features, such as:

1. The target radiate of curvature must be larger than the wavelength λ.
2. The theory yields an infinite result for flat and singly curved surface.
3. The theory fails if the specula point is near an edge.
4. The theory does not take into the account the polarization effect of excited field also the diffracted fields such as the fields in shadow areas.

- **Physical Optics (PO):**

This theory is based on two approximation, they are "tangent plane approximation" and "far field approximation". In the tangent plane approximation the integration element is assumed to be a tangent plane to the incident field. For far field approximation, the gradient of the Green's function is replaced by the Green's function itself multiplied by a constant factor.

The PO technique is more efficient than GO, due to:

1. The simplified integral equation can be evaluated exactly for a few special structures.
2. It has no polarization dependency, since the polarization of the scattered wave is precisely that of the incident wave.
3. The PO technique has a disadvantage; it fails for wide non-specula angles.

- **Geometrical Theory of Diffraction (GTD):**

The theory state that "the incident ray excites a fictitious cone of diffracted rays, all subtend the same angle with respect to the edge as that subtended by the incident ray". This method comes as an extension of GO method to account the non-zero fields in the shadow region, as shown in figure (1.2).

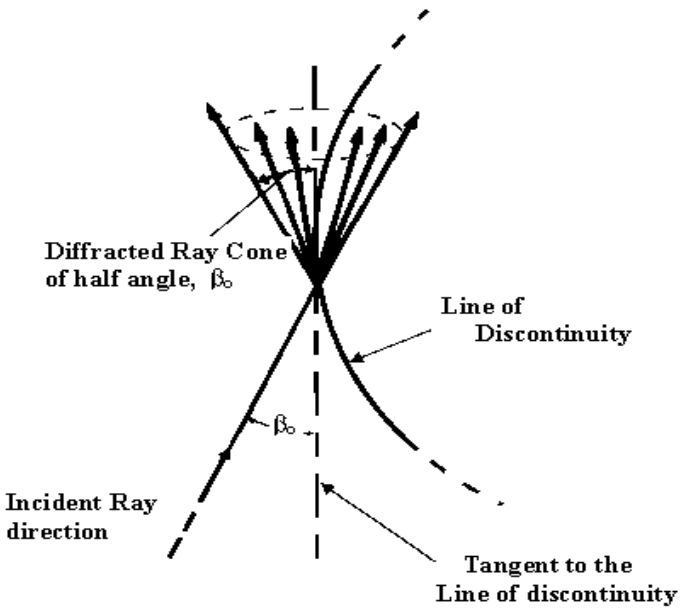

Fig (1.2): Diffracted ray cone from a line of discontinuity

The GTD have some drawbacks:

1. The observation point must be laid within the fictitious Keller cone, otherwise yields precisely zero.
2. The theory predicts infinite fields when the observation point is pierced by infinity of rays, such as point's lies on the axis of body of revolution (BOR).
3. It takes into the account the diffracted fields, such as the fields in the shadow region.
4. The GTD is used to compute the scattered fields well away from the specular direction as well as the polarization effects are inherently built-in.

- **Method of Moments (MoM):**

Method of Moment (MoM) technique is one of the well known methods that are used in electromagnetic scattering problems. This technique is based on reducing the operator equations to a system of linier equations that is written in matrix form.

The features of this method can be summarized in the following:

1. It has a frequency domain RCS prediction technique.
2. It takes to the account the entire electromagnetic phenomenon and also the polarization effects for excite field.
3. It is an integral equation based technique.

One of the advantages of using this method is that the results are very accurate because the equations that his method use is essentially exact and MoM provides a direct numerical solution of these equations. Another advantage is that in practice, it is applicable to geometrically complex scatter [7].

- **Finite Difference – Time Domain (FD - TD):**

This method is a popular computational electrodynamics modelling technique. It is considered easy to understand and easy to implement in software. Since it is a

time-domain method, solutions can cover a wide frequency range with a single simulation run.

The FDTD method belongs in the general class of grid-based differential time-domain numerical modeling methods. The time-dependent Maxwell's equations (in partial differential form) are discredited using central-difference approximations to the space and time partial derivatives. The resulting finite-difference equations are solved in either software or hardware in a leapfrog manner: the electric field vector components in a volume of space are solved at a given instant in time; then the magnetic field vector components in the same spatial volume are solved at the next instant in time; and the process is repeated over and over again until the desired transient or steady-state electromagnetic field behavior is fully evolved.

This method take accounts the polarization effects and the diffracted fields. In addition, the method is a differential equation technique (as mention above).

- **Effective Partial Differential Equation Algorithm (EPDEA):**

This method is used to solve the scattering problems by three dimensional body of revolution using Partial Differential Equation (PDE) technique. This technique is employed in conjunction with a radiation boundary condition applied in the Fresnel region of the scattered. Based on an asymptotic expansion derived by Wilcox, the radiation boundary condition is used to truncate the PDE mesh [4]. More about this method will be discussed later in this thesis.

- **Characteristics Basis Function Method (CBFM):**

This method have been developed in conjunction with the Fast Fourier Transform (FFT) for matrix generation to improve the efficiency of the Method of Moment when analyzing electromagnetic scattering from large Perfect Electrically Conducting (PEC) bodies of revolution. The CBFs are high-level basis functions comprising conventional sub domain bases, and their use leads to a reduced matrix which can be solved by using a direct method. By using this technique, one can get a good advantage that the computational time and memory requirement can be significantly reduced for large BOR problems [5].

The second part, reduction of RCS (RRCS), the information in this technique is limited and it is difficult to obtain as well but due to the development in the semiconductors, the RRCS is taken place in the radar systems [6]. There are four basic techniques for reducing the RCS; they are shaping, radar absorbing materials, passive cancellation and finally the active cancellation. Of course each technique of these has its advantage and disadvantage.

With purpose shaping, the shape of the target's reflecting surfaces is designed such that they reflect energy away from the source. The aim is usually to create a "cone-of-silence" about the target's direction of motion. Due to the energy reflection, this method is defeated by using passive radars. With radar absorbed material (RAM), it can be used in the original construction, or as an addition to highly reflective surfaces. For the passive cancellation, its concept is to generate an echo source whose amplitude and phase can be adjusted to cancel any other echo sources, it calls impedance loading some times. The fourth technique; active cancellation; the target

generates a radar signal equal in intensity but opposite in phase to the predicted reflection of an incident radar signal (similarly to noise cancelling ear phones). This creates destructive interference between the reflected and generated signals, resulting in reduced RCS. To incorporate active cancellation techniques, the precise characteristics of the waveform and angle of arrival of the illuminating radar signal must be known, since they define the nature of generated energy required for cancellation. Except against simple or low frequency radar systems, the implementation of active cancellation techniques is extremely difficult due to the complex processing requirements and the difficulty of predicting the exact nature of the reflected radar signal over a broad aspect of an aircraft, missile or other target. This technique is also called active loading.

As we know, bodies of revolutions objects are used in these problems to simplify the calculations, due to the symmetrical property so the surface current can be explained in some small terms that helps in reducing the memory usage and the computation time. In the same way, complex bodies can be treated like bodies of revolution in their calculations.

This body of revolution (BOR) approach has been applied to several numerical methods such as MoM, EPDEA and CBFM. In our work, we are going to use the Efficient Partial Differential Equation Algorithm EPDEA to calculate the surface current density J_θ.

1.2 Radar Cross Section (RCS):

Radar Cross Section (RCS); σ is the unit of measure of how detectable an object is with radar. For example a stealth aircraft (which is designed to be undetectable) will have design features that give it a low RCS, as opposed to a passenger airliner that will have a high RCS. An object's RCS depends on its size, reflectivity of its surface, and the directivity of the radar reflection caused by the object's geometric shape. So in other expression, RCS can be written as:

Radar Cross Section (RCS) = Geometric Cross Section × Reflectivity × Directivity

Because that RCS is an effective surface area that intercepts the incident wave and that scatters the energy iso-tropically in space, the mathematically expression can be written as:

$$\sigma = 4\pi R^2 \frac{P_s}{P_i} \qquad 1.1$$

Where σ is the RCS, P_s is the scattered power density measured at the target, and P_i is the incident power density seen at a distance R away from the target. Also it is common in electromagnetic analysis to write it as:

$$\sigma = 4\pi R^2 \frac{\left|E_s^{\,2}\right|}{\left|E_i^{\,2}\right|} \qquad 1.2$$

Where E_s^2 and E_i^2 are the scattered and incidents fields respectively. The scattered field from the body is due to presence of the target, so the total field is the incident field E_i added with the scattered field E_s. From this, the returned power P_r is given by:

$$P_R = \left(\frac{P_T G_T}{4\pi R^2}\right)\sigma\left(\frac{1}{4\pi R^2}\right)(A_R) \qquad 1.3$$

Where $\left(\frac{P_T G_T}{4\pi R^2}\right)$ is the power density at the target coming from the transmitters' radiation. Its unit is measured by $watt/m^2$. The term $\sigma\left(\frac{1}{4\pi R^2}\right)$ is the amount of the incident power reflected to the receiver. A_R represents the receiving area of the antenna, figure (1.3).

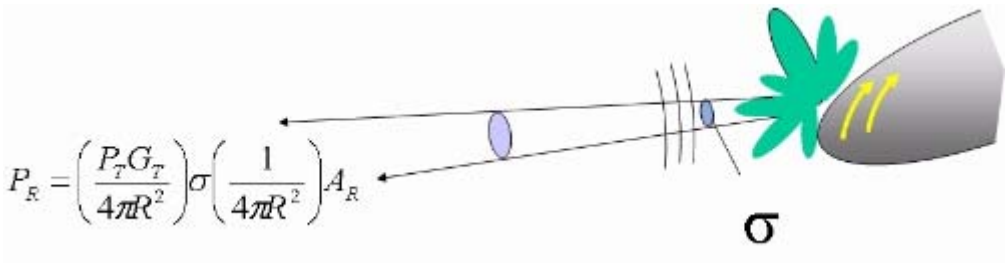

Fig (1.3): The RCS σ and the returned power P_R

The RCS is affected by:

1. Target geometry, its material properties and the orientation relative to the radar.
2. The frequency and waveform of the incident wave.
3. Polarization of incident and scattered wave.
4. Polarization of transmitter and receiver of radar.

These factors must be specified carefully to keep the information from the calculation useful.

In addition, there are other RCS measurements, mono static and bi-static radar cross section terms are commonly used. Mono static RCS measurement is used when the transmitter and receiver are the same type, otherwise bi-static RCS measurement is used when the transmitter and the receiver are isolated and the angle that makes there is called bi-static angle [8].

1.3 Radar Range Equation (RRE):

The radar range equation is developed to establish the radar sensitivity requirements. The far-field conditions are implicit in the radar cross section definition, so that the isolation between the receiver R_x and the transmitter T_x can be determined by the radar range equation to satisfy the above conditions.

The radar range equation (RRE) relates to the power, as show in the equation:

$$P_r = \left(\frac{P_t G_t}{4\pi R^2}\right)\left(\frac{\sigma}{4\pi R^2}\right)\left(\frac{\lambda^2}{4\pi}\right)G_r L = \frac{P_t G_t G_r \left(\sigma/\lambda^2\right)}{(4\pi)^3 \left(R/\lambda\right)^4} L \qquad 1.4$$

Where: P_r is the power available to the radar receiver, P_t is the back power output of the radar transmitter, G_r and G_t are the gain of the receiving and the transmitting antenna respectively, σ is the target radar cross section related to the incident and scattered polarization and radar orientation, λ is the operation wavelength, R is the range separation between target and radar and L is the system losses which include ohmic losses in radar components, propagation losses here is free-space and processing losses [9].

1.4 Scattering Regimes:

From the general definition for scattering problem which is defined as: when an electromagnetic waves incident on an obstacle, it induces surface currents. These currents which can be electric in case of perfect electric conduction and both electric and magnetic in case of dielectrically coated material, radiates and produces a so called "scattered field" and generally it propagate in all directions with various amplitude and phase.

When this scattered field backs toward the radar transmitter the field is called "mono static" signature and the field is called "bi-static" signature when the scattered field in some other direction is desired.

According to the body electrical size the radar cross section (RCS) regimes can be classified into three regions which are [6]:

1. Rayleigh region
2. Resonance (Mie) region
3. Optics region

1.5 Literature Survey:

To demonstrate there are three sub-sections, which are given below:

1.5.1 Scattering and radiation from perfectly conducting bodies.

1.5.2 Scattering and radiation from imperfectly conducting bodies.

1.5.3 Radar Cross Section RCS measurements.

1.5.1 Scattering and radiation from perfectly conducting bodies:

Researchers are having great interest in scattering problem of EM waves by perfectly conducting from irregular geometrical shape. The scattering problem is very complicated boundary-value problem. But in spherical case of scattier with surface coordinate and orthogonal coordinate system the method of separation variables [8] is helpful to solve the vector wave equation.

J.S. YEH et. Al. In 1956, experimentally measured scattering of EM waves by perfectly conducting sphere and dices to figure the echo area and compared with the theoretical formula. Latest computation of scattering functions for conducting sphere [9].

In earlier studies from 1861 to 1941 regarding scattering problems by sphere involved greatest name of mathematical physics. There are some techniques for only bodies (which are smaller in comparison with the wavelength) like variation and quasi-static which are providing good solution for scatter of various shapes. If the diameter or width of scatter is large in comparison with wavelength then there following optical solutions [10]:

1. Physical Optics PO
2. Geometric Optics GO
3. Geometrical Theory of Diffraction

Mogeus G. Andreasen in 1965, solved the general scattering problem by an Integral Equation (IE) method. By this method the electric and magnetic fields interior and exterios to the cylinders with arbitrary cross-sectional shape and arbitrarily varying anisotropic surface impedance. This IE was programmed to a computer [11].

A.Baghdasarian and D.J. Angelakos in 1965, solved an integral equation numerically, in purpose to determine the current distribution and after that the back-scattered pattern for loops as a function of rotation angle [14].

J.R. Mautz and R.F. Harrigton in 1968 and 1969, found the current distribution on the scattier and on aperture antennas, by using the IE formulation for surface current on conducting bodies of revolution (BOR) with MoM as a numerical solution [12, 14].

Nan N. Wang et. al. In 1975, suggested to use a sinusoidal reaction concept to formulate scattering and radiation problems for conducting surface of arbitrary shape. For example, there are rectangular plates and corner reflector antennas [17].

J.R Mautz and R.F. Harrington in 1979, developed a combination of two currents electric and magnetic, also called combined source and it is placed on the surface of the conducting body. It is for EM scattering and radiation from perfectly conducting body [18].

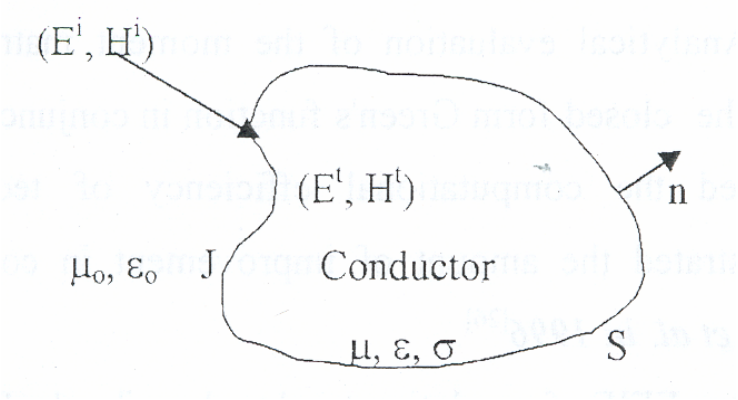

Fig (1.4): Scattering geometry

J.F. Shaeffer and L.N. Medgyesi in 1981 and J.F. Shaeffer in 1982, formulated the scattering and radiation of EM waves from BOR with attached wires even called junction problems. To determine the scattered pattern for multiple wires they had to use the MoM. Currents are represented in three different functions [13, 20].

1. Mode –dependent and piecewise – continuous expansion function on BOR,
2. Piecewise –continuous function on the wire, and
3. A continuity preserving basis functions for the junction region.

To solve the EM scattering problems for perfectly conducting BOR, hybrid solutions combinations are used between MoM and PO, (Physical Optics). Even for scattier in the resonant range the formulation is accurate [21, 22].

Yehuda, et. al. in 1988, studied the convergence of the numerical solution, MoM, with the exact solution by changing the N for perfectly conducting bodies , for example, spheres and rounded cylinder. The number of the basis function N is the main limitation of MoM [23].

Stephen D. Gedney and Rajj Mittra in 1990, tried to find the current distribution on scattier by using fast Fourier transformation FFT combined with the MoM. FFT in Greens function, while source and field points are coinciding, was used to overcome the singularity [24].

L.N. Medgyesi – Mitschang and J.M. Putnam in 1990, compared with their experimental data, the back- scattered cross-section. The aim was to describe the EM scattering from finite planar and curved perfect electrically conducting surface truncated by an irregular edge by using an EFIE formulation. [27].

Lale Alatan et al. in 1996 demonstrated the amount of improvement in computation, where analytical evaluation of the moment matrix elements is found by using the closed-form Greens function in co work with MoM has been improved the computational efficiency of technique singularity.

Via Maxwell's equations and equivalent principle, radiation problem via slot from perfectly conducting bodies of two or three dimensions is formulated. The process is constructed and transformed it to a matrix equation, which is solved by the matrix algorithm with hybrid MoM solution to reduce the computation time and storage media [15 - 18].

IE formulation can solve many problems of scattering and radiation from BOR, aperture antennas, large BOR, and doubly periodic surface are treated by it [19 - 21].

1.5.2 Scattering and radiation from imperfectly conducting bodies:

Most of the researchers of EM discipline are interested in scattering problems of EM waves by irregular shape of imperfectly conducting objects. It is possible to get the analytical solution for spherical and spheroid symmetry [22], as well as for uniform shapes, as for example, spheres or complete cylinders. By the method of separation of variables, a big wave of equations inside and outside the body can be solved. The sum of the given incident fields and the scattered fields are creating the complete field in the exterior region. The equivalent currents are radiated on the scattier.

Te-Kao-Wu and L. Tasi in 1977, have created the arbitrary-shaped lossy-dielectric BOR. They treated it by incorporation the equivalent magnetic current contributions. Two-coupled vector IE may be defined via Maxwell's equation, Green's theorem, and the boundary conditions. By expanding the unknown surface currents in the Fourior decomposition and MoM of Galerkin's approach, the unknown surface can be discovered [23].

A year later in 1978, Ronald J. Pogoraelski created a formula for propagation matrix, where scattering from penetrable objects is a combination between the concept of invariant imbedding and surface equivalent current with the MoM [24].

A simple and efficient method to formulate the EM problem of scattering and radiation from dielectric surfaces was devised by Allen W. G. Glisson and Ronald R. Wilton in 1980. To solve this problem they involved conducting strips (both TE and TM), a bent rectangular plate and conducting and dielectric BOR [25]. Later, Allen W. G. Glisson in 1984, used the equivalence principle to develop a single surface integral equation, for frequency domain problems involving EM scattering from homogenous material bodies. At the body surface, an equivalent current is defined and this is the IE equation [27].

Different cases used with the formulation of imperfectly conducting BOR were shown by Medgyesi et al In 1985. There are impedance boundary condition IBC, resistive sheet boundary condition RBC and magnetically conducting sheet boundary condition MBC. They compared the results with each other and eventually with Mie's solution for impedance coated spheres and MoM for EFIE, MFIE, and CFIE formulations of impedance coated bodies [28]. In 1986 they formulated a combined field integral equation CFIE for EM scattering from perfectly conducting

BOR layered dielectric coatings. Thanks to this type of formulation it is very easy to get unique solutions at all frequencies. The resulting system of IE can be solved by using the MoM [26].

Lossy dielectric BOR was formulated by J. R. Mautz and R. F. Harrigton in 1972 by using the characteristic modes and MoM. Because this method doesn't need a matrix inverse, it reduced the computation time and storage media [29].

The effect of several parameters on the radiation pattern or mode excitation such as micro-strip antennas was studied by L. Shafai and A. A. Kishk in 1986, 1989 and 1989, by applying BOR and MoM. With that they treated multilayered bodies of complex geometries. Eventually, they came to conclusion that this method is very useful [30 - 32]. In 1996 L. Shafai and A. A. Kishk came up with the suggestion to formulate the different formulation into seven different ways. The purpose was to find the surface current by studying the different formulations for scattering from dielectric coated BOR [33].

Another study n 1986 was conducted by Korada V. et al whose purpose was to formulate the three dimensional homogenous Lossy dielectric objects by using the surface triangle patch model. He presented a CFIE with MoM [34].

A terrific agreement between CFBM solution and exact solution for coated cylinders was acquired by Gilles Y. Delisle et al in 1989 and K. L. Wu in 1990. The solution for multiple dielectric conducting cylinders is in coupled finite boundary element method CFBM, which is developed to formulate EM scattering fields [35 - 36].

When the MoM combines with finite element method, a hybrid formulation is made. That is to solve the EM scattering and/or absorption problems, where the inhomogeneous media is involved. By applying the equivalence principle and transform the original problem into interior and exterior problems and that is the basic technique. The exterior problem is solved by the MoM and the interior problem involving inhomogeneous medium is solved by FEM [37].

H. A. Rageb et al. in 1991 found that the solution with theoretical treatment based on the boundary value solution is much more general than the other solutions given before. He came to this conclusion through investigating the scattering properties of dielectric coated non-confocal conducting elliptic cylinders. This solution can handle a variety of scattering geometries [38].

Later in 1996, Schmitz J. L reasoned out the various methods for treating scattering of EM problem from dielectric BOR. With that he got the equivalent surface currents and then the scattering pattern [39].

Recent works by P. Jacobsson and T. Rylander have used the optical theorem to obtain the total scattering cross section from the forward scattering. Mcheney and B. Borden develop a theory based on the classical theory of monostatic backscattering

radar for radar imagining that combines temporal, spectral and spatical Diversity[64–65].

A. Qing[66] used the boundary condition of vanishing tangential electric field on the surfaces of the perfectly conducting cylinders to derive a set of electro field integral equation and solve the scattering problem by point-matching method.

A Hybrid MoM solution of scattering from finite arrays of cylindrical cavities have been used by F.J.Villegas et al[67].

C.L. Rino et al[68] have used the method of ordered multiple interactions for closed bodies where as standard Method of Moments (MoM) can be applied.

1.5.3 Radar Cross Section RCS measurements:

R. F. Harrigton and J. R. Mautz in 1972, gave suggestion for the concept of characteristic modes, which is used to obtain the RCS for loaded bodies. By using exact solution for simple spheres or complex object [17] has developed radar cross-section estimation of objects rather than ‘’simple’’ or ‘’complex’’ [40].

Rajj Mittra and Richard K. in 1989, to estimate RCS for bodies of revolution BOR they used the partial differential equation PDE [41].

Tasy, Win-Jiuun in 1995, Suggested numerical solutions for conducting and dielectric structures of arbitrary cross section the RCS, estimated by MoM [42 - 44] and for complex target the PO and PTD [45].

Many investigators have been used the conjugate gradient method with fast Fourier transformation FFT for two or three-dimension arbitrary and uniform objects [46 - 50].

In newer times, the researches in RCS field are constructed into two-part predication and reduction of RCS for objects. By using different numerical solutions, many new formulations have been performed. As for example, the finite element time domain FE-TD, partially differential equation PDE, finite volume time domain FV-TD, method of moments MoM and hybrid solutions for perfectly conducting, dielectric, coated material and composite bodies [51 - 62]. The IE formulation with MoM is used in this thesis to relate the RCS for BOR of perfectly conducting, dielectric, dielectrically coated material.

CHAPTER TWO

SCATTERING FROM BODIES OF REVOLUTION (BOR)

2.1 Introduction:

To get an exact solution for the problems of the electromagnetic wave scattered by a perfect conducting objects is available only for limited general shapes, such as the common shapes (elliptic, cylindrical and spherical) objects.

Some of these solutions can be complicated in form and calculations. For arbitrarily shaped objects the analytical solutions is not feasible, so in such cases the approximate or numerical solutions must be introduced.

In this thesis, two methods are going to be discussed. One of them is the Method of Moment (MoM) and the second one is Efficient Partial Differential Equation Algorithm (EPDEA).

2.2 Efficient Partial Differential Equation Algorithm (EPDEA):

2.2.1 Introduction:

From the title, we can see that the problem of electromagnetic scattering by a perfect electric conductor (PEC) body of revolution can be solved by the partial differential equations (PDE). This problem is possible to formulate in terms of the components of the electric and magnetic fields in the region surrounding the perfect electric conductor. In this method, two scalar potentials are employed and express all of the six field components in terms of the potentials. As mention in literature survey part, Morgan and Mei have introduced such potential, the coupled azimuthally potentials (CAPs). In the coming part, the formulation of body of revolution is given in more detail [4].

2.2.2 Formulation of Body of Revolution Problem:

The Wilcox representation and the two scalar potentials that are used are $u_m(r,\theta)$ and $v_m(r,\theta)$ which are defined as:

$$E_\phi(r,\theta,\phi) = \sum_{m=-\infty}^{\infty} \psi(r) u_m(r,\theta) e^{jm\phi}$$
$$\eta_0 H_\phi(r,\theta,\phi) = \sum_{m=-\infty}^{\infty} \psi(r) v_m(r,\theta) e^{jm\phi} \qquad 2.1$$

Where:

$$\psi(r) = \frac{e^{-jkr}}{r} \qquad 2.2$$

The other field components which are $E_{r,m}(r,\theta)$, $E_{\theta,m}(r,\theta)$, $H_{r,m}(r,\theta)$ and $H_{\theta,m}(r,\theta)$ can be expressed in terms of the potential u_m and v_m as following:

$$E_{r,m} = jf_m\left(m\sin(\theta)\frac{\partial(r\psi u_m)}{\partial r} - k_0\mu_r r\sin(\theta)\frac{\psi\partial(v_m\sin(\theta))}{\partial\theta}\right) \quad 2.3$$

$$E_{\theta,m} = jf_m\left(\frac{\psi\partial(u_m\sin(\theta))}{\partial\theta} + k_0\mu_r r\sin^2(\theta)\frac{\partial(r\psi v_m)}{\partial r}\right) \quad 2.4$$

$$H_{r,m} = \frac{jf_m}{\eta_0}\left(m\sin(\theta)\frac{\partial(r\psi v_m)}{\partial r} + k_0\varepsilon_r r\sin(\theta)\frac{\psi\partial(u_m\sin(\theta))}{\partial\theta}\right) \quad 2.5$$

$$H_{\theta,m} = \frac{jf_m}{\eta_0}\left(\frac{\psi\partial(v_m\sin(\theta))}{\partial\theta} - k_0\varepsilon_r r\sin^2(\theta)\frac{\partial(r\psi u_m)}{\partial r}\right) \quad 2.6$$

Where $f_m(r,\theta) = (\mu_r(r,\theta)\varepsilon_r(r,\theta)k_0{}^2r^2\sin^2(\theta) - m^2)^{-1}$ 2.7

The advantage of using these potentials in place of E and H is the reducing of the number of unknowns to be dealt with infinite difference or finite element formulations. By substituting these components into Maxwell's equations, we get the following:

$$\begin{aligned}\nabla\cdot E &= \frac{1}{r^2}\frac{\partial}{\partial r}(r^2E_r) + \frac{1}{r\sin(\theta)}\frac{\partial}{\partial\theta}(\sin(\theta)E_\theta) + \frac{1}{r\sin(\theta)}\frac{\partial}{\partial\phi}E_\phi \\ &= \frac{1}{r^2}\frac{\partial}{\partial r}\left(r^2\left[jf_m\left(m\sin(\theta)\frac{\partial(r\psi u_m)}{\partial r} - k_0\mu_r r\sin(\theta)\frac{\psi\partial(v_m\sin(\theta))}{\partial\theta}\right)\right]\right) \\ &+ \frac{1}{r\sin(\theta)}\frac{\partial}{\partial\theta}\left(\sin(\theta)\left[jf_m\left(\frac{\psi\partial(u_m\sin(\theta))}{\partial\theta} + k_0\mu_r r\sin^2(\theta)\frac{\partial(r\psi v_m)}{\partial r}\right)\right]\right) \\ &+ \frac{1}{r\sin(\theta)}\frac{\partial}{\partial\phi}\left(\frac{e^{-jkr}}{r}\sum_{m=-\infty}^{\infty}u_m(r,\theta)e^{jm\phi}\right)\end{aligned} \quad 2.8$$

$$\begin{aligned}\nabla\times H &= \frac{1}{r^2\sin(\theta)}\left[\left(\frac{\partial}{\partial\theta}\left(r\sin(\theta)E_\phi\right)\right) - \frac{\partial}{\partial\phi}(rE_\theta)\right]\hat{r} \\ &+ \frac{1}{r\sin\theta}\left(\frac{\partial}{\partial\phi}E_r - \frac{\partial}{\partial r}\left(r\sin(\theta)E_\phi\right)\right)\hat{\theta} + \frac{1}{r}\left(\frac{\partial}{\partial r}\left(rE_\theta\right) - \frac{\partial}{\partial\theta}E_r\right)\hat{\phi}\end{aligned} \quad 2.9$$

By solving these equations the following pair of coupled partial differential equations in u_m and v_m can be derived:

$$\begin{aligned}A_1u_m + B_1\frac{\partial u_m}{\partial r} + C_1\frac{\partial u_m}{\partial\theta} + D_1\frac{\partial^2u_m}{\partial r^2} + E_1\frac{\partial^2u_m}{\partial\theta^2} + F_1v_m + G_1\frac{\partial v_m}{\partial r} + H_1\frac{\partial v_m}{\partial\theta} = 0 \\ A_2v_m + B_2\frac{\partial v_m}{\partial r} + C_2\frac{\partial v_m}{\partial\theta} + D_2\frac{\partial^2v_m}{\partial r^2} + E_2\frac{\partial^2v_m}{\partial\theta^2} + F_2u_m + G_2\frac{\partial u_m}{\partial r} + H_2\frac{\partial u_m}{\partial\theta} = 0\end{aligned} \quad 2.10$$

where:

$$A_1 = a_1\psi + b_1\frac{\partial\psi}{\partial r} + d_1\frac{\partial^2\psi}{\partial r^2} \quad 2.11$$

$$B_1 = b_1\psi + 2d_1\frac{\partial\psi}{\partial r} \quad 2.12$$

$$C_1 = c_1\psi \quad 2.13$$

$$D_1 = d_1\psi \tag{2.14}$$

$$E_1 = e_1\psi \tag{2.15}$$

$$F_1 = f_1\psi + g_1\frac{\partial\psi}{\partial r} \tag{2.16}$$

$$G_1 = g_1\psi \tag{2.17}$$

$$H_1 = h_1\psi \tag{2.18}$$

$$A_2 = a_2\psi + b_2\frac{\partial\psi}{\partial r} + d_2\frac{\partial^2\psi}{\partial r^2} \tag{2.19}$$

$$B_2 = b_2\psi + 2d_2\frac{\partial\psi}{\partial r} \tag{2.20}$$

$$C_2 = c_2\psi \tag{2.21}$$

$$D_2 = d_2\psi \tag{2.22}$$

$$E_2 = e_2\psi \tag{2.23}$$

$$F_2 = f_2\psi + g_2\frac{\partial\psi}{\partial r} \tag{2.24}$$

$$G_2 = g_2\psi \tag{2.25}$$

$$H_2 = h_2\psi \tag{2.26}$$

$$a_1 = \frac{1}{f_m^2}\left(-jk_0\varepsilon_r r - jk_0 r\cos(\theta)\frac{\partial}{\partial\theta}(\varepsilon_r f_m\sin(\theta)) - jk_0\sin^2(\theta)\frac{\partial}{\partial r}(\varepsilon_r r^2 f_m) + jk_0\varepsilon_r r f_m\sin^2(\theta)\right) \tag{2.27}$$

$$b_1 = \frac{1}{f_m^2}\left(-jk_0 r\sin^2(\theta)\frac{\partial}{\partial r}(\varepsilon_r r^2 f_m) - 2jk_0\varepsilon_r r^2 f_m\sin^2(\theta)\right) \tag{2.28}$$

$$c_1 = \frac{1}{f_m^2}\left(-jk_0 r\sin(\theta)\frac{\partial}{\partial\theta}(\varepsilon_r f_m\sin(\theta)) - 2jk_0\varepsilon_r r f_m\sin(\theta)\cos(\theta)\right) \tag{2.29}$$

$$d_1 = \frac{1}{f_m^2}\left(-jk_0\varepsilon_r r^3 f_m\sin^2(\theta)\right) \tag{2.30}$$

$$e_1 = \frac{1}{f_m^2}\left(-jk_0\varepsilon_r r f_m\sin^2(\theta)\right) \tag{2.31}$$

$$f_1 = \frac{1}{f_m^2}\left(jm\cos(\theta)\frac{\partial}{\partial r}(r f_m) - jm\frac{\partial}{\partial\theta}(f_m\sin(\theta))\right) \tag{2.32}$$

$$g_1 = \frac{1}{f_m^2}\left(-jmr\sin(\theta)\frac{\partial f_m}{\partial\theta}\right) \tag{2.33}$$

$$h_1 = \frac{1}{f_m^2}\left(jmr\sin(\theta)\frac{\partial f_m}{\partial\theta}\right) \tag{2.34}$$

$$a_2 = \frac{1}{f_m^2}\left(jk_0\mu_r r + jk_0 r\cos(\theta)\frac{\partial}{\partial\theta}(\mu_r f_m \sin(\theta)) + jk_0 \sin^2(\theta)\frac{\partial}{\partial r}(\mu_r r^2 f_m) - jk_0\mu_r r f_m \sin^2(\theta)\right) \quad 2.35$$

$$b_2 = \frac{1}{f_m^2}\left(jk_0 r\sin^2(\theta)\frac{\partial}{\partial r}(\mu_r r^2 f_m) + 2jk_0\mu_r r^2 f_m \sin^2(\theta)\right) \quad 2.36$$

$$c_2 = \frac{1}{f_m^2}\left(jk_0 r\sin(\theta)\frac{\partial}{\partial\theta}(\mu_r f_m \sin(\theta)) + 2jk_0\mu_r r f_m \sin(\theta)\cos(\theta)\right) \quad 2.37$$

$$d_2 = \frac{1}{f_m^2}\left(jk_0\mu_r r^3 f_m \sin^2(\theta)\right) \quad 2.38$$

$$e_2 = \frac{1}{f_m^2}\left(jk_0\mu_r r f_m \sin^2(\theta)\right) \quad 2.39$$

$$f_2 = \frac{1}{f_m^2}\left(jm\cos(\theta)\frac{\partial}{\partial r}(r f_m) - jm\frac{\partial}{\partial\theta}(f_m \sin(\theta))\right) \quad 2.40$$

$$g_2 = \frac{1}{f_m^2}\left(- jmr\sin(\theta)\frac{\partial f_m}{\partial\theta}\right) \quad 2.41$$

$$h_2 = \frac{1}{f_m^2}\left(jmr\sin(\theta)\frac{\partial f_m}{\partial\theta}\right) \quad 2.42$$

By following Wilcox representation, an asymptotic representation can be written for u_m and v_m as following:

$$\begin{aligned} u_m(r,\theta) &= \left(A_{0m}(\theta) + \frac{A_{1m}(\theta)}{r} + \frac{A_{2m}(\theta)}{r^2} + \cdots\right) \\ v_m(r,\theta) &= \left(B_{0m}(\theta) + \frac{B_{1m}(\theta)}{r} + \frac{B_{2m}(\theta)}{r^2} + \cdots\right) \end{aligned} \quad 2.43$$

If we consider that the behaviour of the fields is near the outer boundary and this boundary is sufficiently far from the scatterer, the terms of order $\frac{1}{r^2}$ and higher can be negligible contribution to the above u_m and v_m and can be written in a good approximation as following [4]:

$$\begin{aligned} u_m(r,\theta) &= \left(A_{0m}(\theta) + \frac{A_{1m}(\theta)}{r}\right) \\ v_m(r,\theta) &= \left(B_{0m}(\theta) + \frac{B_{1m}(\theta)}{r}\right) \end{aligned} \quad 2.44$$

By using the mesh truncation scheme to solve this problem, we can conclude several important advantages [4]:

1. The truncation scheme does not increase the bandwidth of the finite difference matrix.
2. No complicated three-dimensional vector absorbing boundary condition for the electric and magnetic fields is needed.

3. It is unnecessary to derive Bayliss-Turkel type of boundary conditions for the potentials u_m and v_m.
4. The solutions generated via this truncation scheme appear to exhibit the same order of numerical accuracy as predicted for a second-order Bayliss-Turkel type.
5. This method of truncation is extremely simple to implement numerically.

2.3 Method of Moment (MoM):

2.3.1 Introduction:

There are some solutions are available for the problem of electromagnetic (EM) wave scattered by perfectly conducting objects. These solutions are complicated in calculations and for limited general shapes like elliptic, cylindrical and spherical objects.

In the chapter we will use Electric field integral equation EFIE to formulate the scattering problems bye a conduction bodies of revolution BOR. We will use method of moment (MOM) to solve IE. In this method we will first expand the unknown surface current distribution in series of suitable basis function by this IE could be reduced to the set of simultaneous liner equations. By solving these liner equations we will get surface current distribution.

2.3.2 Formulation of Scattering Problem:

On perfectly conduction body of revolution, the EFIE of electric current $\bar{J}$ induced on surface ***S*** as shown in fig 2.1. The boundary condition that is tangential electric field must be vanishing at surface is stratified by an incident electric field $\bar{E}$ as:

$$-\hat{n}\times\bar{E}^{s}_{\tan}(r)=\hat{n}\times\bar{E}^{inc}_{\tan} \qquad 2.45$$

Where:

$\hat{n}$ is the unit vector normal to the surface ***S***

$\bar{E}^{s}$ is the scattered field due to $\bar{J}$ on ***S***

tan is tangential component on ***S***

The scattered filed produced by equivalent current can be expressed in terms of vector and scalar potentials as:

$$\bar{E}^{s}(r)=-j\omega\bar{A}(r')-\nabla\Phi(r') \qquad 2.46$$

The magnetic vector potential is as:

$$\bar{A}(r') = \frac{\mu}{4\pi}\int_s \bar{J}(r')G(\vec{r},\vec{r}')ds \qquad 2.47$$

Where the Green's function for BOR is as:

$$G(\vec{r},\vec{r}') = \frac{\exp(-jk|\vec{r}-\vec{r}'|)}{|\vec{r}-\vec{r}'|} \qquad 2.48$$

The distance from source point by positional vector $(\vec{r}')$ to the field point $(\vec{r})$ is as:

$$R = |\vec{r}-\vec{r}'| = \sqrt{(\rho-\rho')^2 + (z-z')^2 + 2\rho\rho'(1-\cos(\phi-\phi'))} \qquad 2.49$$

The scalar potential in term of equivalent electric charge distribution is as:

$$\Phi = \frac{1}{4\pi\varepsilon}\int \sigma(\vec{r}')G(\vec{r},\vec{r}')ds \qquad 2.50$$

Where electric charge related to electric current by continuity equation is as:

$$\sigma(\vec{r}') = \frac{-1}{j\omega}\nabla_s \bullet \bar{J}(\vec{r}') \qquad 2.51$$

So equation 2.45 becomes:

$$\hat{n}\times\bar{E}^{inc}_{\tan} = \hat{n}\times\left[\frac{j\omega\mu}{4\pi}\int_s \bar{J}(\vec{r}')G(\vec{r},\vec{r}')ds + \frac{j\nabla}{4\pi\omega\varepsilon}\int_s \nabla'\cdot\bar{J}(\vec{r}')G(\vec{r},\vec{r}')ds\right]_{\tan} \qquad 2.52$$

And equation 2.52 as operator equation is as:

$$\left|L(\bar{J}) = \bar{E}^{inc}\right|_{\tan} \qquad 2.53$$

Where **L** is integro differential operator as:

$$L(\bar{X}) = \int_s j\omega\mu\bar{X}(r')\frac{e^{-jkR}}{4\pi R}ds + \frac{\nabla}{j\omega\varepsilon}\int_s \nabla'\cdot\bar{X}(r')\frac{e^{-jkR}}{4\pi R}ds \qquad 2.54$$

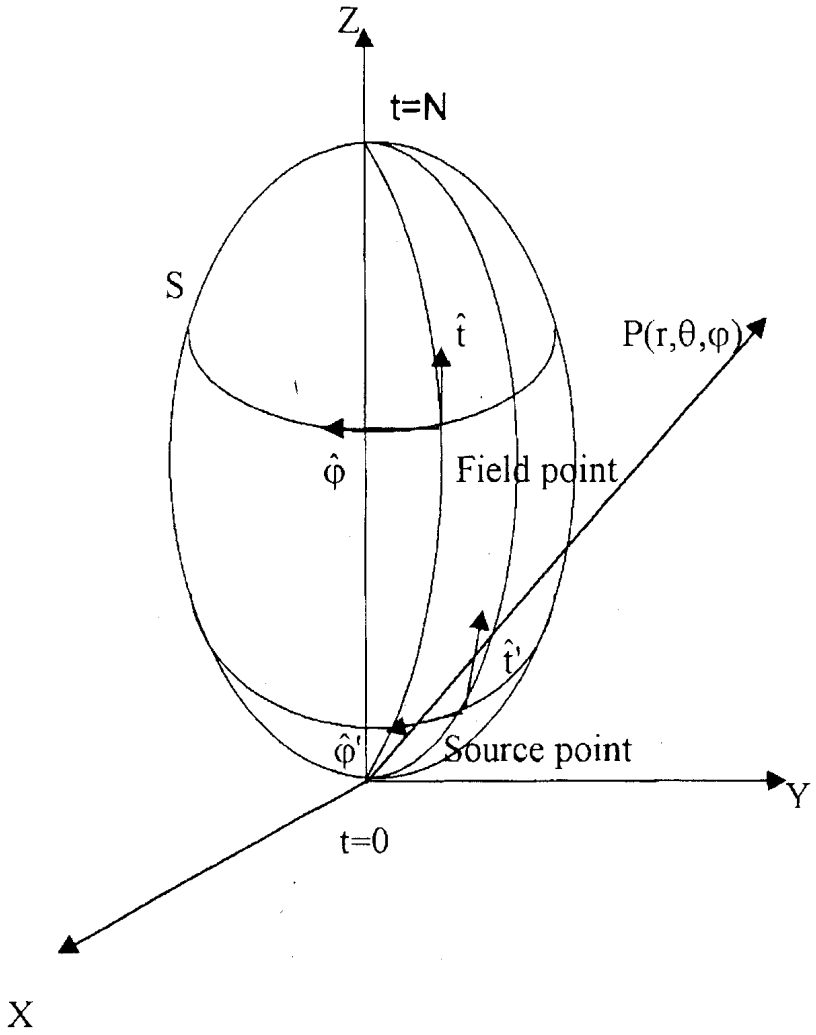

Fig (2.1): Geometry & coordinate system of a BOR.

2.3.3 Moment Solution:

According to Galerkin's approach [12], the numerical method is MOM. This numerical method starts by reducing equation 2.52. The steps involves in MOM are as below

- The first step and main task in MOM solution is to replace perfectly conduction body by equivalent electric surface currents by using the equivalence principle [4].
- The second step is to obtain a set of coupled IE of equivalent current components as in equation 2.52.
- Third step is the final step; this step involves expanding of equivalent surface current in term of finite set of N basis function. Due to rotational symmetry of body we can use Fourier series to represent this function as in equation 2.55

$$\bar{J}(\vec{r}') = \sum_{n,j} I_{nj}^{I} J_{nj}^{I}(\vec{r}')\hat{u}_t' + I_{nj}^{\varphi} J_{nj}^{\varphi}(\vec{r}')\hat{u}_{\varphi}' \qquad 2.55$$

Where:

$$\bar{J}'(\vec{r}') = J_{nj}^{\varphi}(\vec{r}') = \rho' f(t') e^{jn\varphi} \qquad 2.56$$

I_{nj}^{I} and I_{nj}^{φ} are to be determined unknown coefficients where n is summation of Fourier mode and j is summation of basis function. By subdividing BOR in to annular rings and by enforcing N weighted (testing) average of IE the unknown coefficient will be obtained.

$$\overline{W}(\vec{r}) = \sum I_{mj}^{t} W_{mj}^{t}(\vec{r})\hat{u}_t + I_{mj}^{\varphi} W_{mj}^{\varphi}(\vec{r})\hat{u}_{\varphi} \qquad 2.57$$

Where:

$$\overline{W}_{mj}^{t}(\vec{r}) = W_{mj}^{\varphi}(\vec{r}) = \rho f(t) e^{jm\varphi} \qquad 2.58$$

According to Galerkin's approach $W = J^{*}$.

The orthogonal vector to S are $\overline{W}$ and $\bar{J}$. For (n ≠ m) $\overline{W}_{mi}$ is orthogonal to $\bar{J}_{nj}$ over 0 to 2π on φ and all inner products are zero except those for which (n = m). This fact allowed each mode to be treated completely independently of the other mode [30]. The inner product is as:

$$\left\langle \overline{P}, \overline{Q} \right\rangle = \int_s \overline{P} \cdot \overline{Q}\, ds \qquad 2.59$$

Where $\overline{P}$ and $\overline{Q}$ are tangential vectors to S.

The inner Product for BOR is as:

$$\int_s ds \int_s ds' = \int_0^N dt \int_0^{2\pi} \rho d\varphi \int_0^N dt' \int_0^{2\pi} \rho' d\varphi \qquad 2.60$$

The generalized "network type" matrix equation after testing equation 2.52 is as:

$$[Z_n][I_n] = [V_n] \qquad 2.61$$

Where impedance is $[Z_n]$, Excitation is $[V_n]$ and an unknown coefficient is $[I_n]$. Which are as:

$$[Z_n] = \left[\left\langle W_{ni}, L(J_n) \right\rangle\right] \qquad 2.62$$

$$[V_n] = \left[\left\langle W_{ni}', E^{inc} \right\rangle\right], \left[\left\langle W^{\varphi}{}_{ni}, E^{inc} \right\rangle\right] \qquad 2.62a$$

$$[I_n] = [[I'_{ni}], [I^{\varphi}_{ni}]] \qquad 2.62b$$

$[Z_n]$ is impedance matrix of the body as:

$$[Z_n] = \begin{bmatrix} Z^{//}_n & Z^{/\varphi}_n \\ Z^{\varphi/}_n & Z^{\varphi\varphi}_n \end{bmatrix} \qquad 2.63$$

Z sub-matrices given by explicit form [13]:

$$\left(Z^{\alpha\beta}_n\right) = \int_0^N dt \int_0^{2\pi} \rho d\varphi \int_0^N dt' \int_0^{2\pi} \rho' d\varphi' \left\{ j\omega\mu\left(W^{\alpha}_{ni} \cdot J^{\beta}_{nj}\right) + \frac{1}{j\sigma\varepsilon}\left(\nabla \cdot W^{\alpha}_{ni}\right)\left(\nabla' \cdot J^{\beta}_{ni}\right) \right\} G(\vec{r}, \vec{r}') \qquad 2.64$$

Where α and β are combination of t and ϕ directed, n is mode number and moreover

$$\nabla' \cdot J = \frac{1}{\rho'} \frac{\partial}{\partial t'} \left(\rho' J'_{nj} \cdot \hat{u}_t\right) + \frac{1}{\rho'} \frac{\partial}{\partial \varphi'} \left(J^{\varphi}_{nj} \cdot \hat{u}_{\varphi}\right) \qquad 2.65$$

$$\nabla \cdot W = \frac{1}{\rho} \frac{\partial}{\partial t} \left(\rho J W'_{ni} \cdot \hat{u}_t\right) + \frac{1}{\rho} \frac{\partial}{\partial \varphi} \left(W^{\varphi}_{ni} \cdot \hat{u}_{\varphi}\right) \qquad 2.66$$

For evaluation of Z elements, the tangential unit vectors of BOR as in figure 2.1 are as:

$$\hat{u}_t = \sin v \cos\varphi \hat{x} + \sin v \sin\varphi \hat{y} + \cos v \hat{z} \qquad 2.67$$

$$\hat{u}_{\varphi} = -\sin\varphi \hat{x} + \cos\varphi \hat{y} \qquad 2.67a$$

And for field and source point vectors are as:

$$\hat{u}'_t = \sin v' \cos\varphi' \hat{x} + \sin v' \sin\varphi' \hat{y} + \cos v' \hat{z} \qquad 2.68$$

$$\hat{u}'_{\varphi} = -\sin\varphi' \hat{x} + \cos\varphi' \hat{y} \qquad 2.68a$$

$\hat{u}'_{\varphi}$ is always normal to z-axis but $\hat{u}_t$ is at angle v with z-axis. And its positive when $\hat{u}_t$ point away from z-axis and negative if $\hat{u}_t$ toward z-axis.

The Green's function as below may be eliminating ϕ integral in equation 2.64:

$$g_n = 4\pi \int_0^{\pi} \cos n\varphi' \frac{e^{jkR_0}}{R_0} d\varphi' \qquad 2.69$$

R_0 is given with ϕ = 0. And reaming integral in equation 2.64 for t and t' is approximated by triangle function for both current expansion function and testing function as:

$$\rho f_i(t) = T(t - t_i) \tag{2.70}$$

$$T(t) = \begin{cases} 1 - |t| & for\,|t| < 1 \\ 0 & for\,|t| > 1 \end{cases} \tag{2.71}$$

The triangle function as in figure 2.2 is used to represent the current expansion and testing functions.

By using equation 2.65, 2.70 and 2.64 we obtain the explicit form of Z sub-matrices for equation 2.63.

$$\left(Z_n^{tt}\right)_{ij} = \sum_{p=1}^{4} \sum_{q=1}^{4} \left\{ \omega\mu T_p T_q \left[\sin v_p \sin v_q \frac{g_{n+1} - g_{n-1}}{2} + \cos v_p \cos v_q g_n \right] + \frac{1}{j\omega\varepsilon} T_p T_q g_n \right\} \tag{2.72}$$

$$\left(Z_n^{tq}\right)_{ij} = \sum_{p=1}^{4} \sum_{q=1}^{4} \left\{ -\omega\mu T_p T_q \left[\sin v_p \frac{g_{n+1} - g_{n-1}}{2} \right] + \frac{1}{j\omega\varepsilon\rho_q} T_p T_q g_n \right\} \tag{2.72a}$$

$$\left(Z_n^{\varphi t}\right)_{ij} = \sum_{p=1}^{4} \sum_{q=1}^{4} \left\{ \omega\mu T_p T_q \left[\sin v_q \frac{g_{n+1} - g_{n-1}}{2} \right] - \frac{1}{j\omega\varepsilon\rho_p} T_p T_q g_n \right\} \tag{2.72b}$$

$$\left(Z_n^{\varphi\varphi}\right)_{ij} = \sum_{p=1}^{4} \sum_{q=1}^{4} T_p T_q \left[j\omega\mu \frac{g_{n+1} - g_{n-1}}{2} + \frac{1}{j\omega\varepsilon\rho_p\rho_q} g_n \right] \tag{2.72c}$$

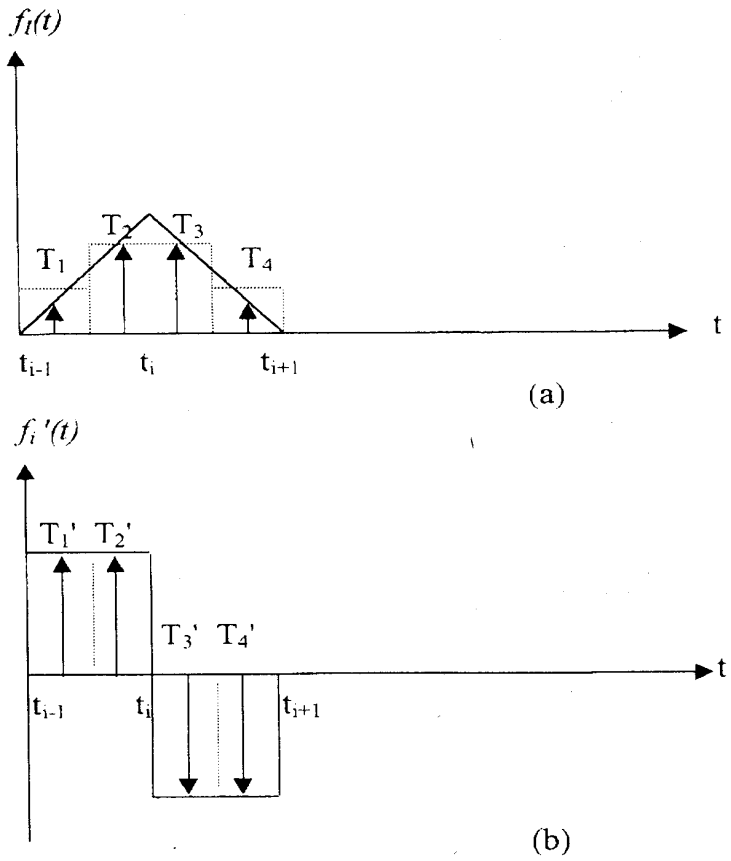

Fig (2.2): (a): Triangle function (solid), four pulses approximation (dashed) and four impulse approximation (arrows).

(b): Derivation of Triangle function (solid), four pulses approximation (dashed) and four impulse approximation (arrows).

Calculation used by Mautz and Harrington[13] to reduce equation 2.69 and with some mathematical manipulation we can get equation 2.73

$$G_n = \frac{\pi}{M}\sum_{m-1}^{M} \cos n\phi_m \, f(\phi_m) \qquad 2.73$$

Where:

$$\phi_m = \left(m - \frac{1}{2}\right)\frac{\pi}{M}$$

M = 2N interval in ϕ directed

$$f(\phi_m) = \exp\left(-jKR_{pq}\right)\left[2\left(1 + jKR_{pq}\right)\ln\frac{t_2 + \left(t_2^2 + d^2\right)^{1/2}}{t_1 + \left(t_1^2 + d^2\right)^{1/2}}\right] \qquad 2.74$$

Where:

$$R_{pq} = \left[\left(\rho_p - \rho_q\right)^2 + 2\rho_p\rho_q\left(1-\cos\phi_m\right) + \left(z_p - z_q\right)\right]^{1/2} \quad 2.75$$

$$\begin{aligned} t_1 &= t_0 - \frac{1}{4} \\ t_2 &= t_0 + \frac{1}{4} \\ t_0 &= \left|\left(z_p - z_q\right)\cos v_q + \left(\rho_p\cos\phi_m - \rho_q\right)\sin v_q\right| \\ d^2 &= R_{pq}^2 - t_0^2 \end{aligned} \quad 2.76$$

Then equation 2.72 becomes

$$\left(Z_n^{tt}\right)_{ij} = \sum_{p=1}^{4}\sum_{q=1}^{4}\left\{\omega\mu T_p T_q\left[\sin v_p \sin v_q \frac{G_{n+1} - G_{n-1}}{2} + \cos v_p \cos v_q G_n\right] + \frac{1}{j\omega\varepsilon}T_p' T_q' G_n\right\} \quad 2.77$$

$$\left(Z_n^{tq}\right)_{ij} = \sum_{p=1}^{4}\sum_{q=1}^{4}\left\{-\omega\mu T_p T_q\left[\sin v_p \frac{G_{n+1} - g_{n-1}}{2}\right] + \frac{1}{j\omega\varepsilon\rho_q}T_p' T_q G_n\right\} \quad 2.77a$$

$$\left(Z_n^{\varphi t}\right)_{ij} = \sum_{p=1}^{4}\sum_{q=1}^{4}\left\{\omega\mu T_p T_q\left[\sin v_q \frac{G_{n+1} - G_{n-1}}{2}\right] - \frac{1}{j\omega\varepsilon\rho_p}T_p T_q' G_n\right\} \quad 2.77b$$

$$\left(Z_n^{\varphi\varphi}\right)_{ij} = \sum_{p=1}^{4}\sum_{q=1}^{4} T_p T_q\left[j\omega\mu\frac{G_{n+1} - G_{n-1}}{2} + \frac{1}{j\omega\varepsilon\rho_p\rho_q}G_n\right] \quad 2.77c$$

2.4 Evaluation of Driving Vector and Far Field components:

The procedure of measurement matrix or linear measurement by J. R. Mautz and R. F. Harrigton is utilized to evaluate the driving vector and the far scattered fields for conduction BOR.

Furthermore; components of the field at a point, voltage along given conductor and current crossing a given surface[63] are linear measurements.

Note: excitation matrix is result from induced current on body surface and measurement matrix is result from far scattered fields produced by induced currents. Examples of linear measurements[46].

- Component of current at some point on S
- Component of field (E or H) at some point in space

So Linear measurement as:

$$\left(V_n\right)=\left\langle \bar{J}_j, \bar{E}^{inc} \right\rangle$$

According to Reciprocity theorem we can find radiation field $\bar{E}^r$ at distance r from origin due to current J on S.

$$\bar{E}^r \cdot \hat{u}_r = \frac{-j\omega\mu}{4\pi r}\exp\left(-jk_0 r\right)\int_s \bar{E}^r \cdot \bar{J}(r')ds \qquad 2.78$$

Where:

$\hat{u}_r$ = unit vector specifying the polarization of the incident wave

$$\bar{E}^r = \hat{u}_r \exp\left(-j\hat{k}\cdot\vec{r}_i\right) \qquad 2.79$$

Equation 2.79 is arbitry plane wave of superposition of two orthogonal components and its unit vectors are as:

$$\hat{u}_r^{\theta} = \cos\theta_r \cos\phi_r \hat{x} + \cos\theta_r \cos\phi_r \hat{y} - \sin\theta_r \hat{z} \qquad 2.80$$

$$\hat{u}_r^{\phi} = \sin\cos\phi_r \hat{x} + \cos\phi_r \hat{y} \qquad 2.80a$$

Where wave number unit vector is $\hat{k} = k.k_0$ in the direction of propagation and vector pointing from origin as in figure 2.3 is $\vec{r}_i$

By using equation 2.79, 2.78, 2.56 and 2.68 we get equation 2.81

$$\bar{E}^i \cdot \hat{u}_r = \frac{-j\omega\mu}{4\pi r}\exp\left(-jk_0 r\right)[R_n][I_n] \qquad 2.81$$

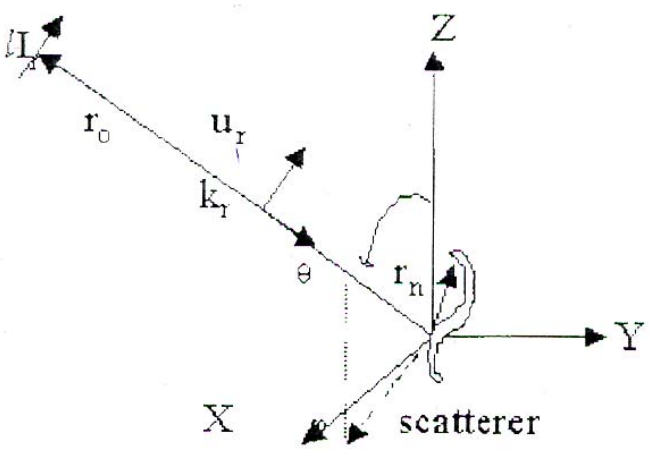

Fig (2.3): Wire scattered and distance dipole.

Where:

$[I_n]$ is coefficient of expansion function and $[R_n]=[[R_n^t],[R_n^\phi]]$

With

$$\begin{aligned}[R_n^t]&=\left[\left\langle \bar{E}^r,\bar{J}_{nj}^t\right\rangle\right]\\ [R_n^\phi]&=\left[\left\langle \bar{E}^r,\bar{J}_{nj}^\phi\right\rangle\right]\end{aligned} \qquad 2.82$$

For Θ polarized plane wave ($\hat{u}_r=\hat{u}_r^\theta$)

$$\begin{aligned}[R_n^{t\theta}]&=\left[\left\langle \bar{E}_\theta^r,\bar{J}_{nj}^t\right\rangle\right]\\ [R_n^{\phi\theta}]&=\left[\left\langle \bar{E}_\theta^r,\bar{J}_{nj}^\phi\right\rangle\right]\end{aligned} \qquad 2.83$$

For ϕ polarized plane wave ($\hat{u}_r=\hat{u}_r^\phi$)

$$\begin{aligned}[R_n^{t\phi}]&=\left[\left\langle \bar{E}_\phi^r,\bar{J}_{nj}^t\right\rangle\right]\\ [R_n^{\phi\phi}]&=\left[\left\langle \bar{E}_\phi^r,\bar{J}_{nj}^\phi\right\rangle\right]\end{aligned} \qquad 2.84$$

By using equation 2.67 and 2.80 we can evaluate the inner product of equation 2.83 and 2.84 the final form is as:

$$J_n(\rho)=\frac{j^n}{2\pi}\int_0^{2\pi}e^{j\rho\cos\alpha}e^{jn\alpha}d\alpha \qquad 2.85$$

And we can also get equation 2.85 [5]

$$\left(R_n^{t\theta}\right)_j=\left\langle \bar{E}_\theta^r,\bar{J}_{nj}^t\right\rangle=\pi j^{n+1}e^{-jn\phi_r}\sum_{p=1}^{4}e^{jkz_p\cos\theta_r}\begin{Bmatrix}\cos\theta_r\sin v_p\left(J_{n+1}(x)-J_{n-1}(x)\right)\\ +2j\sin\theta_{r\cos}v_pJ_n(x)\end{Bmatrix} \qquad 2.86$$

Where $J_n(x)=J_n(k\rho_p\sin\theta_r)$

Normally we are taking $R_n^{t\theta}$ and $R_n^{\phi\phi}$ even in n. And $R_n^{t\phi}$ and $R_n^{\phi\theta}$ odd in n. By comparing equations 2.57 and 2.59 the excitation matrix is differ from measurement matrix in sign of n.

$$\left(V_n^{\alpha\beta}\right)_j=\left(R_n^{\alpha\beta}\right) \qquad 2.87$$

Where:

α and β are replaced as

$$\begin{aligned}
\left(R_n^{t\theta}\right)_i &= \left(R_n^{t\theta}\right) \\
\left(R_n^{\phi\theta}\right)_i &= -\left(R_n^{\phi\theta}\right) \\
\left(R_{-n}^{t\phi}\right)_i &= -\left(R_n^{t\phi}\right) \\
\left(R_n^{\phi\phi}\right)_i &= \left(R_n^{\phi\phi}\right)
\end{aligned} \qquad 2.88$$

So:

$$[I_n] = [Y_n][V_n] \qquad 2.89$$

Where:

$[Y_n]$ is admittance matrix and it is obtained by inverting the Z matrix as:

$$[Y_n] = \begin{bmatrix} Y_n^{tt} & Y_n^{t\phi} \\ Y_n^{\phi t} & Y_n^{\phi\phi} \end{bmatrix} \qquad 2.90$$

And unknown coefficients are as:

$$\begin{bmatrix} I_n^t \\ I_n^\phi \end{bmatrix} = \begin{bmatrix} Y_n^{tt} & Y_n^{t\phi} \\ Y_n^{\phi t} & Y_n^{\phi\phi} \end{bmatrix} \begin{bmatrix} V_n^t \\ V_n^\phi \end{bmatrix} \qquad 2.91$$

So finally far scattered field components E_θ and E_ϕ are as:

$$\begin{bmatrix} E_\theta^s \\ E_\phi^s \end{bmatrix} = \frac{-j\omega\mu}{4\pi r_\theta} e^{jk_\theta r_\theta} \begin{bmatrix} R_{nj}^{t\theta} & R_{nj}^{t\phi} \\ R_{nj}^{t\phi} & R_{nj}^{\phi\phi} \end{bmatrix} \begin{bmatrix} I_{nj}^t \\ I_{nj}^\phi \end{bmatrix} \qquad 2.92$$

2.5 Radar Cross Section (RCS):

Radar cross section is the measure of a target's ability to reflect radar signals in the direction of the radar receiver. It's a property of target having effective area (A_C). The available power at the terminal of receiving antenna is the product of incident power density and effective area. Also we can say power scattered by the target is the product of an effective area and incident power density.

Parameters which are effecting to the RCS are as:

- The frequency of operation.
- The polarization of the transmitting antenna.
- The polarization of receiving antenna.
- The orientation of object relative to the antenna.
- Object or target shape.
- The material of object or target.

So RCS is as:

$$\sigma = 4\pi R^2 \left| \frac{E^s}{E^i} \right|^2 \tag{2.93}$$

Where E^s is scattered field of two components [14]:

$$\begin{bmatrix} E_\theta^s \\ E_\phi^s \end{bmatrix} = \frac{e^{jkr}}{r} \begin{bmatrix} S^{\theta\theta} & S^{\theta\phi} \\ S^{\phi\theta} & S^{\phi\phi} \end{bmatrix} \begin{bmatrix} E_\theta^i \\ E_\phi^t \end{bmatrix} \tag{2.94}$$

By using equation 2.94 in 2.93 then we get

$$\sigma^{pq} = 4\pi \left| S^{pq} \right|^2 \tag{2.95}$$

$$\sigma^{pq} = \frac{-j\omega\mu}{4\pi} \left[\left[R_n^{tp} \right] \left[R_n^{\phi p} \right] \right] \begin{bmatrix} \left[Y_n^{tt} \right] & \left[Y_n^{t\phi} \right] \\ \left[Y_n^{\phi t} \right] & \left[Y_n^{\phi\phi} \right] \end{bmatrix} \begin{bmatrix} V_n^{tq} \\ V_n^{\phi q} \end{bmatrix} \tag{2.96}$$

Where p and q are $\Theta\Theta$, $\phi\Theta$, $\Theta\phi$ and $\phi\,\phi$.

RCS measured in Θ polarized recover with ϕ=0 plane as:

$$\sigma^{\theta\theta} = 16\pi \left| S_1^{\theta\theta} \right|^2 \cos^2 \phi_r \tag{2.97}$$

RCS measured in ϕ polarized recover with $\phi = \pi/2$ plane as:

$$\sigma^{\phi\theta} = 16\pi \left| S_1^{\phi\theta} \right|^2 \cos^2 \phi_r \tag{2.98}$$

For axially incident plane where n= $\pm$1 are excited, so RCS components in horizontal polarization and the vertical polarization are [14]

By using equation 2.96, the scattered field components are as:

$$E_\theta^s = 2 \left(\frac{\exp(-jkr_0)}{r_0} \right) S_1^{\theta\theta} \sin \phi_r \tag{2.99}$$

$$E_\theta^s = 2j \left(\frac{\exp(-jkr_0)}{r_0} \right) S_1^{\phi\theta} \sin \phi_r \tag{2.100}$$

CHAPTER THREE

RESULTS AND DISCUSSION

3.1 Introduction:

In this part, some applications and results will be discussed and shown as a part of the final work. In chapter two, two methods were chosen of several methods to solve the electromagnetic wave scattered by a perfect conducting. The calculation for Efficient Partial Differential Equation Algorithm (EPDEA) is shown in the appendix and is done by mathematica program.

Equation (2.77) for the calculation of the impedance elements is quite difficult because of the complexity of the formulas. An approximate evaluation can be done to reduce the number of the integrations in equation (2.77). For the "t" integration, the $T(t-t_j)$ function is approximated by four pulses of amplitudes $\frac{1}{4},\frac{3}{4},\frac{3}{4},\frac{1}{4}$, as shown in figure (2.2a). The derivative of the $T(t-t_j)$ is represented exactly by four pulses of amplitude 1, 1, -1, -1 as shown in figure (2.2b). The functions ρ, $\sin(v)$, and $\cos(v)$ are assumed constant over each pulse, equal to the values at the midpoint of the pulse. For the t' integration, the $T(t'-t'_j)$ function is approximated by four impulse functions, of strengths $\frac{1}{8},\frac{3}{8},\frac{3}{8},\frac{1}{8}$, as shown in figure (2.2a). The derivative of the $T(t'-t'_j)$ is approximated by four impulse function of strengths $\frac{1}{2},\frac{1}{2},-\frac{1}{2},-\frac{1}{2}$, as shown in figure (2.2b). The functions ρ', $\sin(v')$, and $\cos(v')$ are assumed constant over each pulse. We now define the numbers:

$$\begin{aligned} T_1 &= \frac{1}{8} \qquad T_1' = \frac{1}{2} \\ T_2 &= \frac{3}{8} \qquad T_2' = \frac{1}{2} \\ T_3 &= \frac{3}{8} \qquad T_3' = -\frac{1}{2} \\ T_4 &= \frac{1}{8} \qquad T_4' = -\frac{1}{2} \end{aligned} \tag{3.1}$$

The midpoint of the pulses:

$$t_p = j + \frac{p-2.5}{2} \qquad t_q = i + \frac{p-2.5}{2} \tag{3.2}$$

In terms of these definitions and approximations and using the relationships $\omega\,\mu_a = K_a\eta_a$ and $\omega\,\varepsilon_a = K_a/\eta_a$, the matrix elements of the equation (2.77) reduce to:

$$\left(Z_n^{tt}\right)_{ji}^{JE} = -jK_a\eta_a \sum_{p=1}^{4}\sum_{q=1}^{4}\left\{T_p(t)T_q(t')\left[\sin v_p \sin v_q G_2 + \cos v_p \cos v_q G_1\right] - \frac{1}{jK_a^2}T_p'(t')T_q'(t')G_1\right\} \quad 3.3a$$

$$\left(Z_n^{t\phi}\right)_{ji}^{JE} = -K_a\eta_a \sum_{p=1}^{4}\sum_{q=1}^{4}\left\{T_p(t)T_q(t')\sin v_p G_3 + \frac{n}{K_a^2}\frac{T_q(t')}{\rho_q}T_p'(t)G_1\right\} \quad 3.3b$$

$$\left(Z_n^{\phi t}\right)_{ji}^{JE} = K_a\eta_a \sum_{p=1}^{4}\sum_{q=1}^{4}\left\{T_p(t)T_q(t')\sin v_q G_3 + \frac{n}{K_a^2}T_q'(t')\frac{T_p(t)}{\rho_q}G_1\right\} \quad 3.3c$$

$$\left(Z_n^{\varphi\varphi}\right)_{ji}^{JE} = -jK_a\eta_a \sum_{p=1}^{4}\sum_{q=1}^{4}T_p(t)T_q(t')\left[G_2 - \frac{n^2}{K_a^2\rho_p\rho_q}G_1\right] \quad 3.3d$$

Here ρ_p, ρ_q, v_p, v_q are the ρ and v evaluated at t_p and t_q respectively. Finally, the integrals of equation (2.73) for the Green function must be calculated numerically, and this can be done by using Gauss quadrature.

The Green functions of equation (2.73) have been calculated first for a sphere of radius $(0, 2\lambda)$ as shown in figure (3.1).

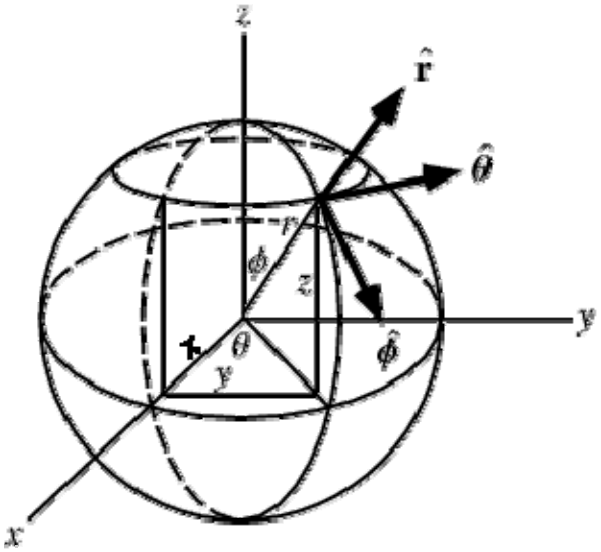

Fig (3.1): Conducting sphere of radius $(0, 2\lambda)$

These calculations are shown in Table [1]. Table [1] also shows the calculations for the impedance Z. To check the accuracy of our calculations, the impedance for current on a sphere has been compared in Table [3.2] with the results of Mautz and Harrington [14, 15, 29, 40]. Table [3.2] shows a very good agreement of our results with the available results of Mautz and Harrington [14, 15, 29, 40].

Table [3.3] shows the generalized admittance matrix elements calculated using $[Y]=[Z]^{-1}$. This matrix will be used in another program to calculate the coefficients of the current distributions J_T and J_ϕ using equation (2.55).

These data are shown in Table (3.4), and has been compared with the results of Mautz and Harrington [14] in figures (3.2), (3.3), (3.4) and (3.5). A very good agreement between our results with other published results can be seen.

Table 3.1: Green functions G and the impedance Z calculation:

12.76	-1.237	4.200	-1.221	2.266	-1.190	1.424	-1.145	0.9256	-1.089
0.5880	-1.023	0.3421	0.9506	0.1562	0.8744	0.1351	0.7969	0.9662	0.7204
0.1812	0.6470	0.2454	0.5784	0.2935	0.5158	0.3289	0.4602	0.3544	0.4121
0.3722	0.3719	0.3843	0.3398	0.3921	0.3157	0.3967	0.2997	0.3988	0.2917
4.346	-1.222	5.392	-1.205	2.548	-1.176	1.509	-1.133	0.9670	-1.078
0.6142	-1.015	0.3617	0.9450	0.1724	0.8712	0.2742	0.7959	0.8446	0.7215
0.1706	0.6498	0.2363	0.5827	0.2858	0.5212	0.3225	0.4665	0.3491	0.4190
0.3679	0.3793	0.3808	0.3474	0.3893	0.3235	0.3943	0.3077	0.3967	0.2997
2.295	-1.191	2.590	-1.176	3.456	-1.148	1.774	-1.108	1.068	-1.058
0.6723	0.9992	0.4031	0.9340	0.2057	0.8648	0.5575	0.7939	0.5983	0.7234
0.1491	0.6553	0.2178	0.5910	0.2701	0.5318	0.3093	0.4789	0.3383	0.4327
0.3591	0.3939	0.3737	0.3627	0.3834	0.3392	0.3893	0.3236	0.3921	0.3157
1.434	-1.146	1.522	-1.133	1.793	-1.109	2.507	-1.073	1.312	-1.029
0.7809	0.9761	0.4727	0.9176	0.2587	0.8552	0.9970	0.7906	0.2208	0.7260
0.1164	0.6629	0.1895	0.6029	0.2459	0.5473	0.2890	0.4971	0.3213	0.4530
0.3451	0.4157	0.3621	0.3855	0.3737	0.3627	0.3808	0.3475	0.3842	0.3398
0.9309	-1.089	0.9727	-1.079	1.075	-1.059	1.323	-1.029	1.943	0.9910
1.012	0.9463	0.5876	0.8963	0.3375	0.8422	0.1619	0.7858	0.3020	0.7286
0.7140	0.6722	0.1507	0.6179	0.2125	0.5671	0.2605	0.5206	0.2973	0.4795
0.3249	0.4444	0.3451	0.4157	0.3591	0.3940	0.3679	0.3793	0.3721	0.3720
0.5910	-1.024	0.6173	-1.016	0.6757	0.9998	0.7850	0.9765	1.019	0.9466
1.584	0.9107	0.8127	0.8702	0.4585	0.8259	0.2486	0.7791	0.9987	0.7308

0.1253	0.6825	0.1000	0.6353	0.1688	0.5905	0.2228	0.5489	0.2650	0.5117
0.2972	0.4795	0.3212	0.4531	0.3382	0.4328	0.3490	0.4191	0.3543	0.4122
0.3439	0.9512	0.3636	0.9456	0.4051	0.9345	0.4749	0.9181	0.5902	0.8966
0.8170	0.8704	1.348	0.8401	0.6817	0.8065	0.3754	0.7702	0.1932	0.7321
0.6351	0.6932	0.3540	0.6543	0.1130	0.6167	0.1744	0.5813	0.2228	0.5490
0.2604	0.5207	0.2889	0.4972	0.3093	0.4790	0.3224	0.4666	0.3288	0.4603
0.1574	0.8749	0.1736	0.8717	0.2069	0.8653	0.2600	0.8556	0.3390	0.8425
0.4602	0.8262	0.6845	0.8066	1.198	0.7841	0.5999	0.7591	0.3262	0.7320
0.1634	0.7034	0.4683	0.6741	0.4250	0.6449	0.1129	0.6168	0.1687	0.5906
0.2124	0.5672	0.2458	0.5474	0.2700	0.5320	0.2857	0.5214	0.2934	0.5160
0.1429	0.7973	0.2821	0.7964	0.5655	0.7944	0.1005	0.7910	0.1628	0.7861
0.2495	0.7793	0.3765	0.7704	0.6016	0.7591	1.108	0.7457	0.5553	0.7300
0.3036	0.7126	0.1540	0.6938	0.4693	0.6741	0.3524	0.6544	0.9981	0.6355
0.1505	0.6181	0.1893	0.6031	0.2176	0.5912	0.2361	0.5829	0.2452	0.5787
0.9611	0.7208	0.8394	0.7218	0.5931	0.7238	0.2155	0.7263	0.3073	0.7289
0.1004	0.7310	0.1938	0.7323	0.3268	0.7321	0.5561	0.7301	1.066	0.7262
0.5415	0.7203	0.3038	0.7127	0.1636	0.7035	0.6381	0.6933	0.1220	0.6827
0.7107	0.6724	0.1160	0.6632	0.1488	0.6555	0.1702	0.6502	0.1808	0.6474
0.1808	0.6474	0.1702	0.6501	0.1488	0.6555	0.1160	0.6632	0.7107	0.6724
0.1220	0.6827	0.6381	0.6933	0.1636	0.7035	0.3038	0.7127	0.5415	0.7203
1.066	0.7262	0.5561	0.7301	0.3268	0.7321	0.1938	0.7323	0.1004	0.7310
0.3073	0.7289	0.2155	0.7263	0.5931	0.7238	0.8393	0.7219	0.9611	0.7208
0.2452	0.5787	0.2361	0.5829	0.2176	0.5912	0.1893	0.6031	0.1505	0.6181
0.9981	0.6355	0.3524	0.6544	0.4693	0.6741	0.1540	0.6938	0.3036	0.7126
0.5553	0.7300	1.108	0.7457	0.6016	0.7591	0.3765	0.7704	0.2495	0.7793
0.1628	0.7861	0.1005	0.7910	0.5655	0.7944	0.2823	0.7964	0.1429	0.7973
0.2934	0.5160	0.2857	0.5214	0.2700	0.5320	0.2458	0.5474	0.2124	0.5672
0.1687	0.5906	0.1129	0.6168	0.4250	0.6449	0.4683	0.6741	0.1634	0.7034
0.3262	0.7320	0.5999	0.7591	1.198	0.7841	0.6845	0.8066	0.4602	0.8262
0.3390	0.8425	0.2600	0.8556	0.2069	0.8653	0.1736	0.8717	0.1574	0.8749
0.3288	0.4603	0.3224	0.4666	0.3093	0.4790	0.2889	0.4972	0.2604	0.5207
0.2228	0.5490	0.1744	0.5813	0.1130	0.6167	0.3540	0.6543	0.6351	0.6932

0.1932	0.7321	0.3754	0.7702	0.6817	0.8065	1.348	0.8401	0.8170	0.8704
0.5902	0.8966	0.4749	0.9181	0.4051	0.9345	0.3636	0.9457	0.3439	0.9512
0.3543	0.4122	0.3490	0.4191	0.3382	0.4328	0.3212	0.4531	0.2972	0.4795
0.2650	0.5117	0.2228	0.5489	0.1688	0.5905	0.1000	0.6353	0.1253	0.6825
0.9987	0.7308	0.2486	0.7791	0.4585	0.8259	0.8127	0.8702	1.584	0.9107
1.019	0.9466	0.7850	0.9765	0.6757	0.9998	0.6173	-1.016	0.5910	-1.024
0.3721	0.3720	0.3679	0.3793	0.3591	0.3940	0.3451	0.4157	0.3249	0.4444
0.2973	0.4795	0.2605	0.5206	0.2125	0.5671	0.1507	0.6179	0.7140	0.6722
0.3020	0.7286	0.1619	0.7858	0.3375	0.8422	0.5876	0.8963	1.012	0.9463
1.943	0.9910	1.323	-1.029	1.075	-1.059	0.9727	-1.079	0.9309	-1.089
0.3842	0.3398	0.3808	0.3474	0.3737	0.3627	0.3621	0.3855	0.3451	0.4157
0.3213	0.4530	0.2890	0.4971	0.2459	0.5473	0.1895	0.6029	0.1164	0.6629
0.2208	0.7260	0.9970	0.7906	0.2587	0.8552	0.4727	0.9176	0.7809	0.9761
1.312	-1.029	2.507	-1.073	1.793	-1.109	1.522	-1.133	1.434	-1.146
0.3921	0.3157	0.3893	0.3235	0.3834	0.3392	0.3737	0.3627	0.3591	0.3939
0.3383	0.4327	0.3093	0.4789	0.2701	0.5318	0.2178	0.5910	0.1491	0.6553
0.5983	0.7234	0.5575	0.7939	0.2057	0.8648	0.4031	0.9340	0.6723	0.9992
1.068	-1.058	1.774	-1.108	3.456	-1.148	2.590	-1.176	2.295	-1.191
0.3967	0.2997	0.3943	0.3077	0.3893	0.3236	0.3808	0.3474	0.3679	0.3793
0.3491	0.4190	0.3225	0.4665	0.2858	0.5212	0.2363	0.5827	0.1705	0.6498
0.8444	0.7215	0.2745	0.7959	0.1724	0.8712	0.3617	0.9450	0.6142	-1.015
0.9671	-1.078	1.509	-1.133	2.548	-1.176	5.392	-1.205	4.346	-1.222
0.3988	0.2917	0.3967	0.2997	0.3921	0.3157	0.3843	0.3398	0.3722	0.3719
0.3544	0.4121	0.3289	0.4602	0.2935	0.5158	0.2454	0.5784	0.1812	0.6470
0.9662	0.7204	0.1351	0.7969	0.1562	0.8744	0.3421	0.9506	0.5880	-1.023
0.9256	-1.089	1.424	-1.145	2.266	-1.190	4.200	-1.221	12.76	-1.237

Z1											
53.46	-2477.	44.61	720.4	32.93	260.0	20.78	95.16	10.24	52.17	2.491	37.39
-2.342	32.88	-4.859	32.25	-5.911	32.68						
44.45	707.3	39.96	-1334.	32.26	413.2	23.45	182.9	14.73	76.37	7.100	47.40
1.234	36.85	-2.690	33.21	-4.858	32.25						
32.95	262.9	32.15	408.1	30.37	-962.5	26.19	324.3	20.30	158.8	13.48	72.10
6.763	46.93	1.237	36.86	-2.337	32.89						
20.81	95.56	23.44	183.9	26.13	322.2	27.15	-811.7	24.92	294.6	19.96	153.1
13.49	72.14	7.108	47.44	2.502	37.42						
10.26	52.28	14.74	76.52	20.29	159.2	24.91	293.9	26.80	-768.9	24.91	293.9
20.29	159.2	14.74	76.52	10.26	52.28						
2.502	37.42	7.108	47.44	13.49	72.14	19.96	153.1	24.92	294.6	27.15	811.7
26.13	322.2	23.44	183.9	20.81	95.56						
-2.337	32.89	1.237	36.86	6.763	46.93	13.48	72.10	20.30	158.8	26.19	324.3
30.37	-962.5	32.15	408.1	32.95	262.9						
-4.858	32.25	-2.690	33.21	1.234	36.85	7.100	47.40	14.73	76.37	23.45	182.9
32.26	413.2	39.96	-1334.	44.45	707.3						
-5.911	32.68	-4.860	32.24	-2.342	32.88	2.491	37.39	10.24	52.17	20.78	95.16
32.93	260.0	44.61	720.4	53.46	-2477.						
Z2											
-1551.	54.68	371.7	50.24	86.50	43.28	44.68	35.22	37.17	27.15	35.32	19.90
34.48	14.01	33.79	9.763	33.28	7.221						
-769.1	45.11	-180.7	41.49	174.2	36.17	63.52	29.77	41.64	23.24	36.24	17.27
34.17	12.35	33.05	8.734	32.41	6.547						
-195.7	32.13	-291.0	29.63	-55.37	26.00	128.3	21.65	57.89	17.02	40.84	12.67
35.54	8.988	33.22	6.222	32.13	4.518						
-81.33	18.80	-100.8	17.26	-168.0	14.91	-17.79	12.07	116.8	9.019	58.76	6.009
42.75	3.371	37.26	1.341	34.96	0.6597						
-46.57	7.677	-52.14	6.529	-69.02	4.732	-126.4	2.466	0.4545	0.1132	126.4	2.466
69.02	-4.732	52.14	-6.529	46.57	-7.677						
-34.96	0.6578	-37.26	-1.341	-42.75	-3.371	-58.76	-6.009	-116.8	-9.019	17.79	12.07
168.0	-14.91	100.8	-17.26	81.33	-18.80						
-32.13	-4.518	-33.22	-6.222	-35.54	-8.988	-40.84	-12.67	-57.89	-17.02	-128.3	21.65
55.37	-26.00	291.0	-29.63	195.7	-32.13						
-32.41	-6.547	-33.05	-8.734	-34.17	-12.35	-36.24	-17.27	-41.64	-23.24	-63.52	29.77
-174.2	-36.17	180.7	-41.49	769.1	-45.11						
-33.28	-7.221	-33.79	-9.764	-34.48	-14.01	-35.32	-19.90	-37.17	-27.15	-44.68	35.23
-86.50	-43.28	-371.7	-50.24	1551.	-54.68						

Z3											
1569.	-54.88	758.4	-45.05	193.8	-32.05	80.96	-18.75	46.46	-7.653	34.93	.7325E
32.12	4.519	32.41	6.547	33.28	7.222						
-370.3	-50.31	184.8	-41.58	289.6	-29.62	100.3	-17.23	52.02	-6.510	37.23	1.348
33.21	6.224	33.05	8.737	33.79	9.768						
-86.91	-43.31	-173.9	-36.22	56.65	-26.04	167.6	-14.91	68.86	-4.720	42.71	3.380
35.53	8.994	34.16	12.35	34.47	14.02						
-44.68	-35.26	-63.63	-29.80	-128.2	-21.68	18.23	-12.09	126.3	-2.462	58.71	6.018
40.83	12.68	36.23	17.28	35.31	19.91						
-37.15	-27.17	-41.63	-23.26	-57.91	-17.04	-116.7	-9.032	0.8807	0.1252	116.7	9.032
57.91	17.04	41.63	23.26	37.15	27.17						
-35.31	-19.91	-36.23	-17.28	-40.83	-12.68	-58.71	-6.018	-126.3	2.462	-18.23	12.09
128.2	21.68	63.63	29.80	44.68	35.26						
-34.48	-14.02	-34.16	-12.35	-35.53	-8.994	-42.71	-3.380	-68.86	4.720	-167.6	14.91
-56.65	26.04	173.9	36.22	86.91	43.31						
-33.79	-9.767	-33.05	-8.737	-33.21	-6.224	-37.23	-1.348	-52.02	6.510	-100.3	17.23
-289.6	29.62	-184.8	41.58	370.3	50.31						
-33.28	-7.222	-32.41	-6.547	-32.12	-4.519	-34.93	0.7345	-46.47	7.653	-80.96	18.75
-193.8	32.05	-758.5	45.05	-1569.	54.88						
Z4											
57.67	-2641.	52.71	-264.4	45.69	-61.31	37.53	-37.68	29.26	-34.35	21.76	34.27
15.61	-34.35	11.13	-34.18	8.428	-33.94						
52.66	-267.8	49.14	-176.2	43.74	-54.78	37.19	-30.95	30.27	-29.88	23.68	31.54
18.04	-32.99	13.77	-33.82	11.13	-34.19						
45.68	-61.62	43.73	-54.99	40.56	-28.89	36.37	-16.08	31.51	-21.69	26.47	26.76
21.80	-30.51	18.04	-32.99	15.61	-34.36						
37.53	-37.73	37.19	-30.98	36.37	-16.07	34.83	2.746	32.51	-5.667	29.59	19.25
26.47	-26.76	23.68	-31.54	21.76	-34.27						
29.26	-34.37	30.27	-29.88	31.51	-21.68	32.51	-5.656	32.90	9.467	32.51	5.656
31.51	-21.68	30.27	-29.88	29.26	-34.37						
21.76	-34.27	23.68	-31.54	26.47	-26.76	29.59	-19.25	32.51	-5.667	34.83	2.746
36.37	-16.07	37.19	-30.98	37.53	-37.73						
15.61	-34.36	18.04	-32.99	21.80	-30.51	26.47	-26.76	31.51	-21.69	36.37	16.08
40.56	-28.89	43.73	-54.99	45.68	-61.62						
11.13	-34.18	13.77	-33.82	18.04	-32.99	23.68	-31.54	30.27	-29.88	37.19	30.95
43.74	-54.78	49.14	-176.2	52.66	-267.8						
8.428	-33.94	11.13	-34.18	15.61	-34.35	21.76	-34.27	29.26	-34.35	37.53	37.68
45.69	-61.31	52.71	-264.4	57.67	-2641.						

Table 3.2: The impedance $Z(\Omega)$ elements on a sphere of radius $(0, 2\lambda)$:

Impedance Element	*Our Results*	*Reference Results[14]*
Z_{11}^{tt}	53.46 – j2477	53.36 – j1904
Z_{55}^{tt}	26.80 – j768.9	26.83 – j701.0
Z_{15}^{tt}	10.26 + j52.28	10.08 + j52.36
$Z_{11}^{\phi\phi}$	57.67 – j2641	57.36 – j2236
$Z_{55}^{\phi\phi}$	32.90 + j9.467	32.93 + j11.05
$Z_{15}^{\phi\phi}$	29.26 – j34.36	29.27 – j34.32
$Z_{11}^{t\phi}$	1569 – j54.88	1100 – j55.08
$Z_{55}^{t\phi}$	$(-1.68 + j0.343)*10^{-4}$	$(-2.12 + j0.405)*10^{-5}$
$Z_{15}^{t\phi}$	-37.15 – j27.17	-37.13 – j27.25

Table 3.3: The generalized admittance matrix $[Y](\Omega^{-1})$:

Y1											
0.3630E-04	-0.1602E-02	0.5820E-04	-0.4313E-03	0.5949E-04	0.1440E-03	0.4360E-04	-0.3064E-03	0.1936E-04	0.2109E-04	-0.2337E-05	-0.1297E-03
-0.1513E-04	0.2210E-05	-0.1718E-04	-0.7370E-04	-0.1087E-04	0.8885E-04						
0.5759E-04	-0.4297E-03	0.9620E-04	-0.4419E-03	0.1053E-03	-0.3705E-03	0.8639E-04	-0.5316E-04	0.5012E-04	-0.2126E-03	0.1222E-04	-0.7892E-04
-0.1442E-04	-0.1056E-03	-0.2375E-04	-0.1337E-04	-0.1693E-04	-0.7436E-04						
0.5876E-04	0.1515E-03	0.1049E-03	-0.3712E-03	0.1269E-03	-0.4147E-04	0.1196E-03	-0.2268E-03	0.8816E-04	-0.8841E-04	0.4484E-04	-0.1642E-03
0.6785E-05	-0.9457E-04	-0.1436E-04	-0.1055E-03	-0.1482E-04	0.3456E-05						
0.4313E-04	-0.3103E-03	0.8620E-04	-0.5167E-04	0.1196E-03	-0.2281E-03	0.1328E-03	0.2438E-03	0.1205E-03	-0.1497E-03	0.8590E-04	-0.7541E-04
0.4478E-04	-0.1645E-03	0.1220E-04	-0.7832E-04	-0.2203E-05	-0.1305E-03						
0.1922E-04	0.2523E-04	0.4995E-04	-0.2131E-03	0.8805E-04	-0.8821E-04	0.1204E-03	-0.1499E-03	0.1341E-03	0.3588E-03	0.1204E-03	-0.1499E-03
0.8805E-04	-0.8822E-04	0.4994E-04	-0.2131E-03	0.1921E-04	0.2524E-04						
-0.2203E-05	-0.1305E-03	0.1220E-04	-0.7832E-04	0.4478E-04	-0.1645E-03	0.8590E-04	-0.7541E-04	0.1205E-03	-0.1497E-03	0.1328E-03	0.2438E-03
0.1196E-03	-0.2281E-03	0.8620E-04	-0.5167E-04	0.4312E-04	-0.3103E-03						
-0.1482E-04	0.3454E-05	-0.1436E-04	-0.1055E-03	0.6785E-05	-0.9457E-04	0.4484E-04	-0.1642E-03	0.8816E-04	-0.8841E-04	0.1196E-03	-0.2268E-03
0.1269E-03	-0.4147E-04	0.1049E-03	-0.3712E-03	0.5875E-04	0.1515E-03						
-0.1693E-04	-0.7436E-04	-0.2375E-04	-0.1337E-04	-0.1442E-04	-0.1056E-03	0.1222E-04	-0.7891E-04	0.5012E-04	-0.2126E-03	0.8638E-04	-0.5316E-04
0.1053E-03	-0.3705E-03	0.9620E-04	-0.4419E-03	0.5759E-04	-0.4297E-03						
-0.1087E-04	0.8885E-04	-0.1718E-04	-0.7370E-04	-0.1513E-04	0.2211E-05	-0.2338E-05	-0.1297E-03	0.1936E-04	0.2109E-04	0.4360E-04	-0.3064E-03
0.5949E-04	0.1440E-03	0.5820E-04	-0.4313E-03	0.3630E-04	-0.1602E-02						
Y2											
0.1646E-02	0.3722E-04	-0.6392E-02	0.5859E-04	0.4903E-02	0.6932E-04	-0.3836E-02	0.6051E-04	0.2336E-02	0.5220E-04	-0.1599E-02	0.3935E-04
0.9627E-03	0.3115E-04	-0.5331E-03	0.2105E-04	0.7572E-04	0.1125E-04						
0.4137E-03	0.5873E-04	0.9168E-03	0.9430E-04	-0.3702E-02	0.1111E-03	0.1864E-02	0.9791E-04	-0.1605E-02	0.8234E-04	0.8067E-03	0.6146E-04
-0.6478E-03	0.4852E-04	0.2596E-03	0.3165E-04	-0.6570E-04	0.1779E-04						
-0.1004E-03	0.5931E-04	0.1907E-02	0.9994E-04	-0.4047E-03	0.1126E-03	-0.2265E-02	0.1023E-03	0.7881E-03	0.8160E-04	-0.9142E-03	0.5741E-04
0.3260E-03	0.4455E-04	-0.3250E-03	0.2555E-04	-0.3041E-05	0.1616E-04						
0.2872E-03	0.4274E-04	-0.8422E-03	0.7768E-04	0.2504E-02	0.8042E-04	-0.4017E-03	0.7280E-04	-0.2151E-02	0.5084E-04	0.7298E-03	0.2599E-04
-0.8830E-03	0.1616E-04	0.2162E-03	0.4665E-06	-0.1229E-03	0.3734E-05						
-0.4700E-05	0.1798E-04	0.8233E-03	0.3815E-04	-0.8927E-03	0.3088E-04	0.2374E-02	0.2302E-04	0.9361E-08	0.6021E-08	-0.2374E-02	-0.2303E-04
0.8927E-03	-0.3087E-04	-0.8233E-03	-0.3817E-04	0.4703E-05	-0.1798E-04						
0.1229E-03	-0.3735E-05	-0.2162E-03	-0.4622E-06	0.8830E-03	-0.1616E-04	-0.7298E-03	-0.2598E-04	0.2151E-02	-0.5084E-04	0.4017E-03	-0.7280E-04
-0.2504E-02	-0.8041E-04	0.8422E-03	-0.7769E-04	-0.2872E-03	-0.4273E-04						
0.3044E-05	-0.1616E-04	0.3250E-03	-0.2555E-04	-0.3260E-03	-0.4455E-04	0.9142E-03	-0.5742E-04	-0.7880E-03	-0.8159E-04	0.2265E-02	-0.1023E-03
0.4048E-03	-0.1126E-03	-0.1907E-02	-0.9995E-04	0.1004E-03	-0.5930E-04						
0.6571E-04	-0.1780E-04	-0.2596E-03	-0.3165E-04	0.6478E-03	-0.4852E-04	-0.8067E-03	-0.6146E-04	0.1605E-02	-0.8233E-04	-0.1864E-02	-0.9792E-04
0.3702E-02	-0.1111E-03	-0.9168E-03	-0.9432E-04	-0.4137E-03	-0.5872E-04						
-0.7572E-04	-0.1125E-04	0.5331E-03	-0.2103E-04	-0.9627E-03	-0.3117E-04	0.1599E-02	-0.3933E-04	-0.2336E-02	-0.5221E-04	0.3836E-02	-0.6051E-04
-0.4903E-02	-0.6932E-04	0.6392E-02	-0.5858E-04	-0.1646E-02	-0.3721E-04						

Y3											
-0.1650E-02	-0.3725E-04	-0.4173E-03	-0.5935E-04	0.9465E-04	-0.6004E-04	-0.2850E-03	-0.4315E-04	0.1324E-05	-0.1805E-04	-0.1226E-03	0.3955E-05
-0.3969E-05	0.1653E-04	-0.6533E-04	0.1808E-04	0.7613E-04	0.1125E-04						
0.6438E-02	-0.5655E-04	-0.9059E-03	-0.9189E-04	-0.1889E-02	-0.9791E-04	0.8290E-03	-0.7604E-04	-0.8098E-03	-0.3779E-04	0.2137E-03	0.1090E-06
-0.3215E-03	0.2465E-04	0.2591E-03	0.3063E-04	-0.5381E-03	0.2013E-04						
-0.5002E-02	-0.6888E-04	0.3707E-02	-0.1126E-03	0.4010E-03	-0.1145E-03	-0.2495E-02	-0.8142E-04	0.8818E-03	-0.3094E-04	-0.8808E-03	0.1670E-04
0.3257E-03	0.4552E-04	-0.6504E-03	0.4933E-04	0.9822E-03	0.3112E-04						
0.3923E-02	-0.5933E-04	-0.1884E-02	-0.9586E-04	0.2271E-02	-0.1008E-03	0.4019E-03	-0.7196E-04	-0.2368E-02	-0.2294E-04	0.7305E-03	0.2543E-04
-0.9174E-03	0.5650E-04	0.8158E-03	0.6024E-04	-0.1636E-02	0.3837E-04						
-0.2400E-02	-0.5188E-04	0.1620E-02	-0.8337E-04	-0.7961E-03	-0.8261E-04	0.2151E-02	-0.5142E-04	-0.7363E-08	-0.4215E-08	-0.2151E-02	0.5142E-04
0.7961E-03	0.8261E-04	-0.1620E-02	0.8336E-04	0.2400E-02	0.5188E-04						
0.1636E-02	-0.3838E-04	-0.8158E-03	-0.6024E-04	0.9174E-03	-0.5650E-04	-0.7305E-03	-0.2543E-04	0.2368E-02	0.2294E-04	-0.4019E-03	0.7196E-04
-0.2271E-02	0.1009E-03	0.1884E-02	0.9587E-04	-0.3923E-02	0.5932E-04						
-0.9822E-03	-0.3113E-04	0.6504E-03	-0.4932E-04	-0.3257E-03	-0.4552E-04	0.8808E-03	-0.1671E-04	-0.8818E-03	0.3093E-04	0.2495E-02	0.8142E-04
-0.4010E-03	0.1144E-03	-0.3707E-02	0.1126E-03	0.5002E-02	0.6889E-04						
0.5381E-03	-0.2013E-04	-0.2591E-03	-0.3064E-04	0.3215E-03	-0.2466E-04	-0.2137E-03	-0.1068E-06	0.8098E-03	0.3780E-04	-0.8290E-03	0.7605E-04
0.1889E-02	0.9792E-04	0.9059E-03	0.9191E-04	-0.6438E-02	0.5655E-04						
-0.7613E-04	-0.1126E-04	0.6533E-04	-0.1808E-04	0.3968E-05	-0.1653E-04	0.1226E-03	-0.3956E-05	-0.1328E-05	0.1805E-04	0.2850E-03	0.4315E-04
-0.9465E-04	0.6004E-04	0.4173E-03	0.5935E-04	0.1650E-02	0.3725E-04						
Y4											
0.3829E-04	-0.1231E-02	0.6013E-04	0.5636E-02	0.7185E-04	-0.4170E-02	0.6310E-04	0.3319E-02	0.5471E-04	-0.1995E-02	0.4144E-04	0.1380E-02
0.3256E-04	-0.8248E-03	0.2204E-04	0.4594E-03	0.1163E-04	-0.6498E-04						
0.5794E-04	0.5654E-02	0.9626E-04	-0.2767E-01	0.1288E-03	0.2989E-01	0.1242E-03	-0.1999E-01	0.1108E-03	0.1358E-01	0.8692E-04	-0.8456E-02
0.6434E-04	0.5520E-02	0.4122E-04	-0.2812E-02	0.2106E-04	0.4616E-03						
0.7152E-04	-0.4235E-02	0.1352E-03	0.3013E-01	0.1715E-03	-0.4857E-01	0.1962E-03	0.4095E-01	0.1824E-03	-0.2524E-01	0.1485E-03	0.1680E-01
0.1082E-03	-0.1039E-01	0.6712E-04	0.5570E-02	0.3253E-04	-0.8375E-03						
0.6171E-04	0.3378E-02	0.1223E-03	-0.2026E-01	0.1947E-03	0.4112E-01	0.2196E-03	-0.5381E-01	0.2356E-03	0.4246E-01	0.1965E-03	-0.2564E-01
0.1463E-03	0.1688E-01	0.8666E-04	-0.8573E-02	0.4034E-04	0.1405E-02						
0.5441E-04	-0.2040E-02	0.1152E-03	0.1379E-01	0.1808E-03	-0.2540E-01	0.2390E-03	0.4252E-01	0.2517E-03	-0.5426E-01	0.2389E-03	0.4252E-01
0.1809E-03	-0.2540E-01	0.1152E-03	0.1379E-01	0.5441E-04	-0.2040E-02						
0.4034E-04	0.1405E-02	0.8665E-04	-0.8572E-02	0.1463E-03	0.1688E-01	0.1966E-03	-0.2564E-01	0.2356E-03	0.4246E-01	0.2197E-03	-0.5381E-01
0.1947E-03	0.4112E-01	0.1224E-03	-0.2026E-01	0.6170E-04	0.3378E-02						
0.3254E-04	-0.8375E-03	0.6706E-04	0.5570E-02	0.1083E-03	-0.1039E-01	0.1484E-03	0.1680E-01	0.1824E-03	-0.2524E-01	0.1961E-03	0.4095E-01
0.1715E-03	-0.4857E-01	0.1351E-03	0.3013E-01	0.7153E-04	-0.4235E-02						
0.2106E-04	0.4616E-03	0.4127E-04	-0.2812E-02	0.6428E-04	0.5520E-02	0.8700E-04	-0.8456E-02	0.1107E-03	0.1358E-01	0.1242E-03	-0.1999E-01
0.1287E-03	0.2989E-01	0.9631E-04	-0.2768E-01	0.5794E-04	0.5654E-02						
0.1163E-04	-0.6498E-04	0.2202E-04	0.4594E-03	0.3258E-04	-0.8248E-03	0.4142E-04	0.1380E-02	0.5472E-04	-0.1995E-02	0.6309E-04	0.3319E-02
0.7185E-04	-0.4170E-02	0.6013E-04	0.5636E-02	0.3829E-04	-0.1231E-02						

Table 3.4: Real and Imaginary parts of T and ϕ directed current. T is the arc length

T	$REAL\ J_T$	$IMAG\ J_T$	$REAL\ J_\phi$	$IMAG\ J_\phi$
0.5	0.02760	2.49E-02	-1.56E-04	4.51E-04
1	0.02790	3.13E-02	-3.79E-04	3.66E-04
1.5	0.01640	2.93E-02	-5.64E-04	2.15E-04
2	0.02070	2.44E-02	-6.62E-04	-6.77E-05
2.5	0.08310	1.88E-02	-6.64E-04	3.20E-04
3	0.00063	1.17E-02	-5.22E-04	7.86E-04
3.5	-0.00541	2.81E-03	-2.34E-04	7.33E-04
4	-0.00944	-4.33E-03	2.21E-04	-1.75E-03
4.5	-0.01110	-9.82E-03	8.11E-04	7.87E-04
5	-0.00943	-1.31E-02	1.52E-03	-4.11E-03
5.5	-0.00564	-1.33E-02	2.33E-03	-6.56E-03
6	-0.00086	-1.10E-02	3.22E-03	-1.47E-02
6.5	0.00454	-6.11E-03	4.00E-03	-4.03E-02
7	0.00933	1.32E-03	4.71E-03	-7.23E-02
7.5	0.01310	1.33E-02	5.84E-03	2.70E-01
8	0.01460	3.98E-02	7.44E-03	-4.76E-01
8.5	0.01420	1.66E-02	7.21E-03	2.88E-01
9	0.11100	7.18E-03	5.42E-03	-7.70E-02
9.50E+00	0.00459	2.30E-03	2.05E-03	4.55E-02

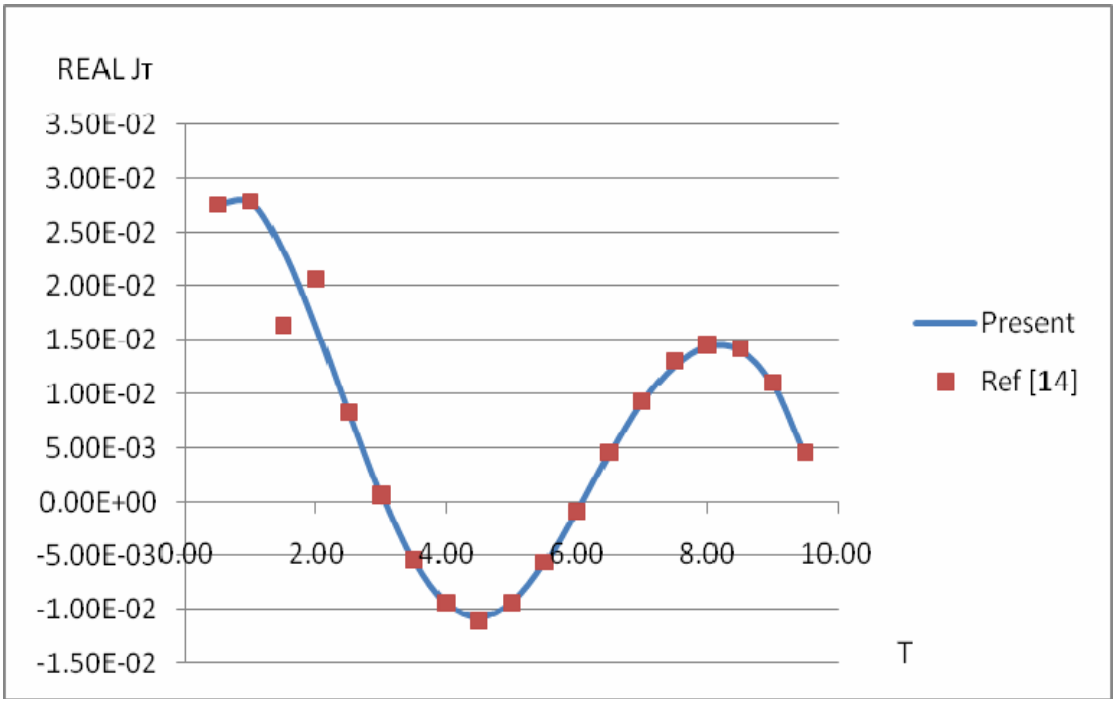

Figure (3.2): The relation between the Real parts of the current J_T with the arc length T

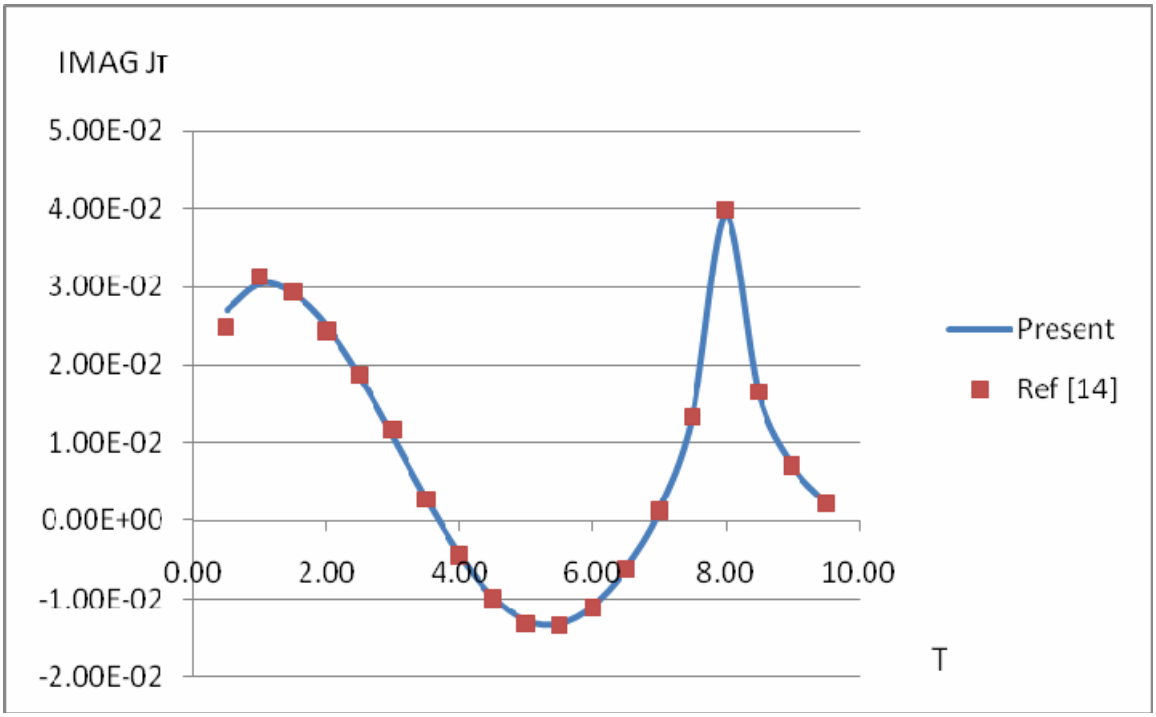

Figure (3.3): The relation between the Imaginary part of J_T and the arc length T

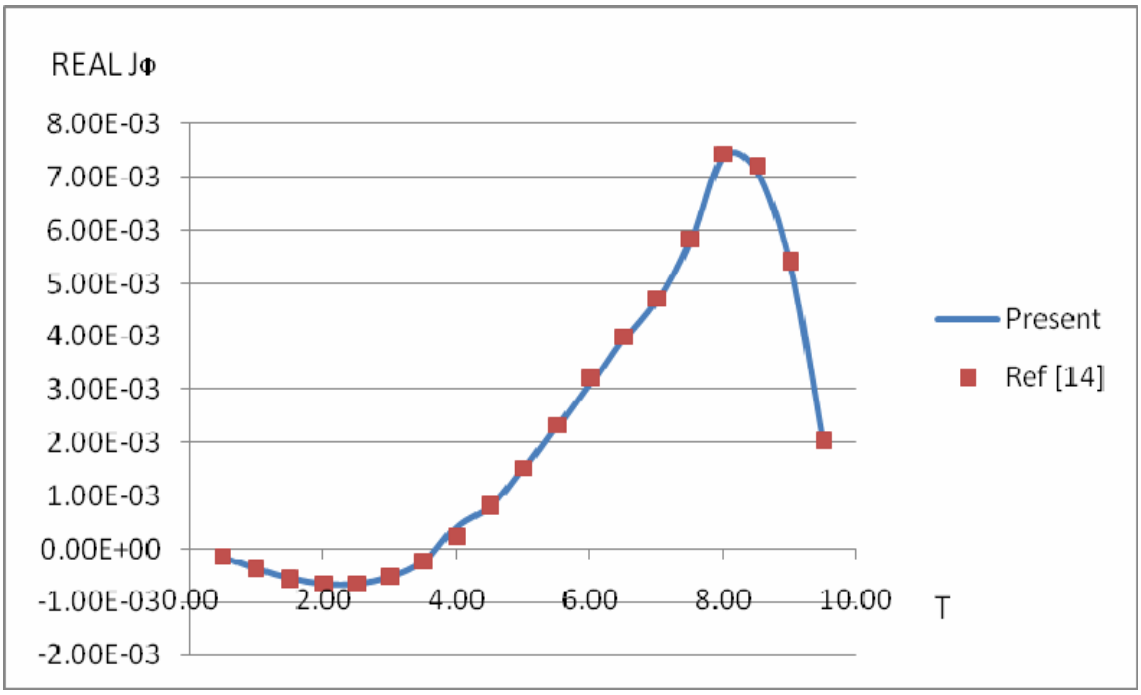

Figure (3.4): The relation between the real part of J_ϕ with the arc length T

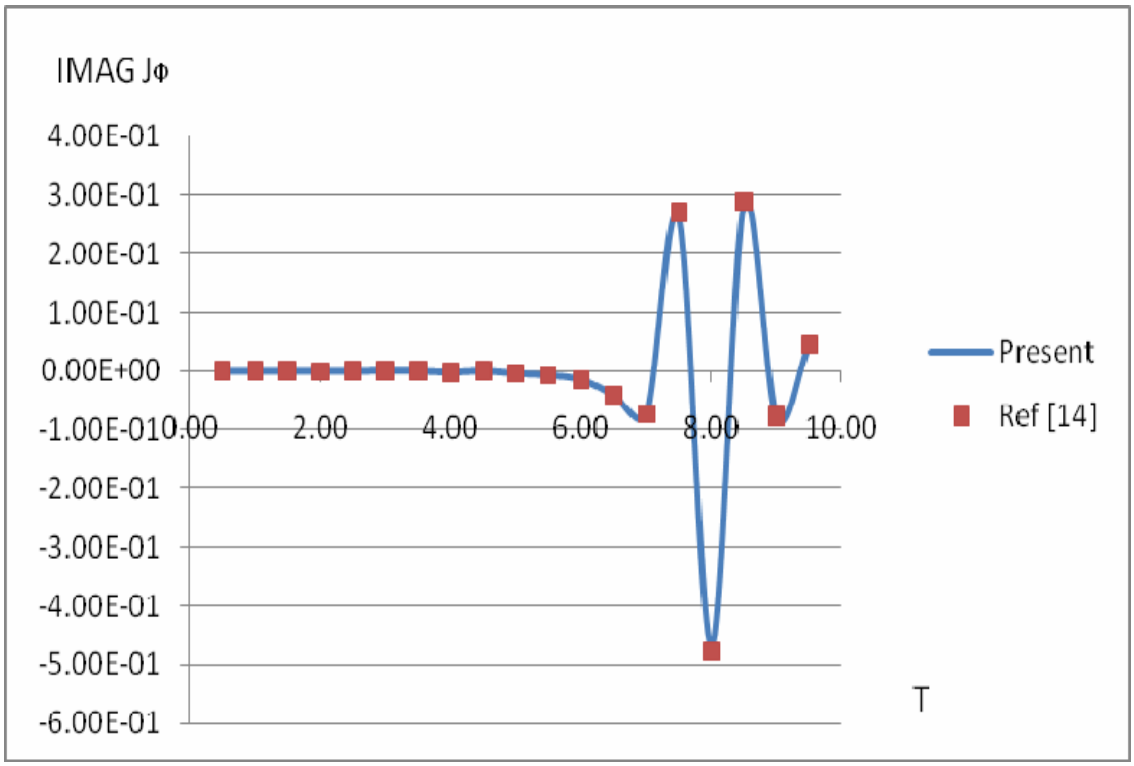

Figure (3.5): The relation between the Imaginary part of J_ϕ with the arc length T

In Table (3.5), the normalized data for the power gain pattern G_θ, E_θ, G_ϕ and E_ϕ are given. These data are also compared with other results in figures (3.6), (3.7), (3.8) and (3.9) with a good agreement.

Table 3.5: The normalized power gain pattern

θ	G_θ	E_θ	G_ϕ	E_ϕ
0	0	0	0	0
5	0.042	0.231	0.037	0.171
10	0.16	0.42	0.121	0.342
15	0.344	0.601	0.243	0.5
20	0.566	0.761	0.427	0.565
25	0.822	0.914	0.619	0.782
30	1.027	1.014	0.799	0.893
35	1.234	1.125	0.969	0.997
40	1.243	1.138	1.102	1.076
45	1.117	1.069	1.256	1.11
50	0.898	0.0944	1.389	1.14
55	0.594	0.777	1.39	1.178
60	0.346	0.599	1.391	1.182
65	0.286	521	1.392	1.183
70	0.39	0.633	1.365	1.174
75	0.701	0.844	1.346	1.16
80	1.077	1.051	1.32	1.145
85	1.376	1.158	1.277	1.137
90	1.422	1.16	1.217	1.104
95	1.3	1.2	1.186	1.084
100	0.877	0.933	1.121	1.06
105	0.499	0.71	1.054	1.032
110	0.311	0.567	1	1.016
115	0.416	0.679	0.98	0.998
120	0.783	0.921	0.934	0.973
125	1.4	1.15	0.884	0.94
130	1.88	1.374	0.833	0.912
135	2.244	1.465	0.785	0.906
140	2.346	1.558	0.679	0.842
145	2.69	1.518	0.612	0.788
150	2.198	1.425	0.517	0.711
155	1.536	1.369	0.414	0.625
160	1.087	1.129	0.282	0.522
165	0.671	0.82	0.166	0.418
170	0.321	0.566	0.078	0.283
175	0.052	0.293	0.025	0.143
180	0	0	0	0

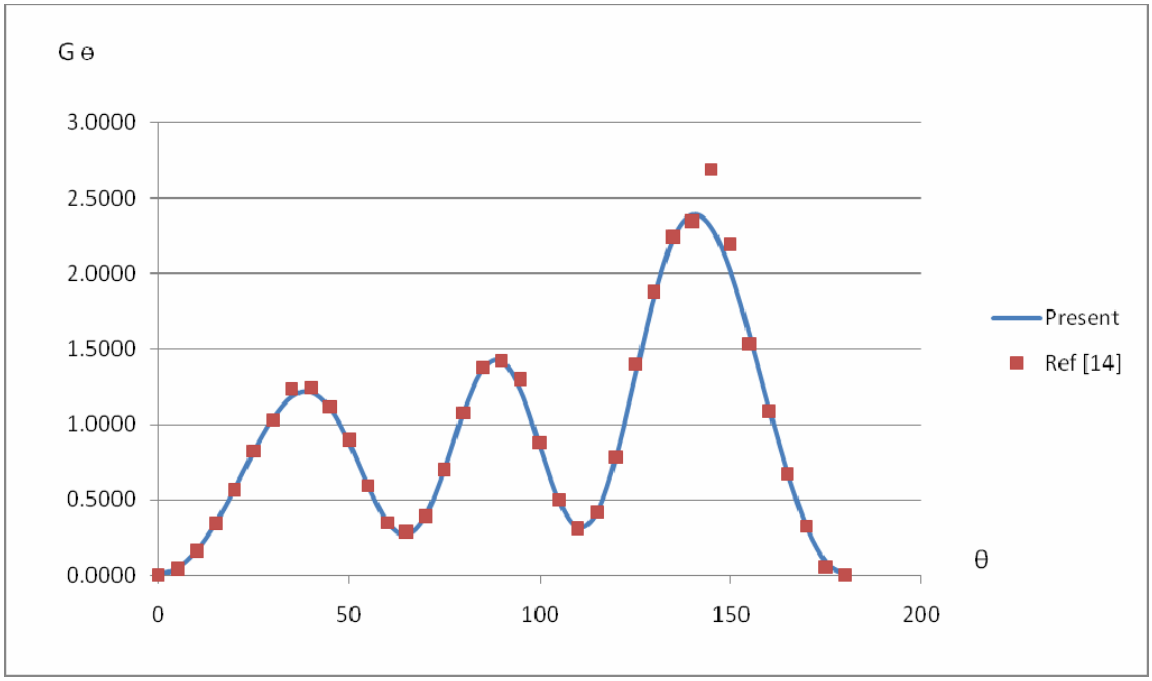

Figure (3.6): The normalized power gain G_θ as a function of θ

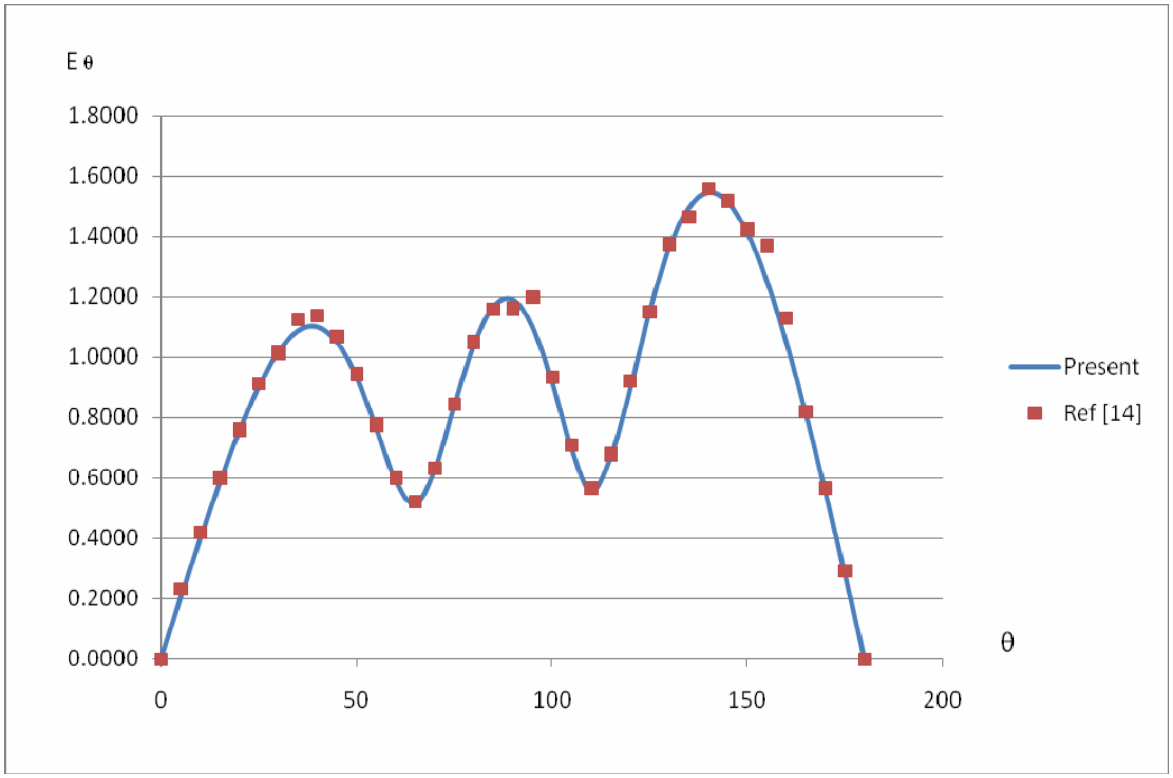

Figure (3.7): The normalized power gain E_θ as a function of θ

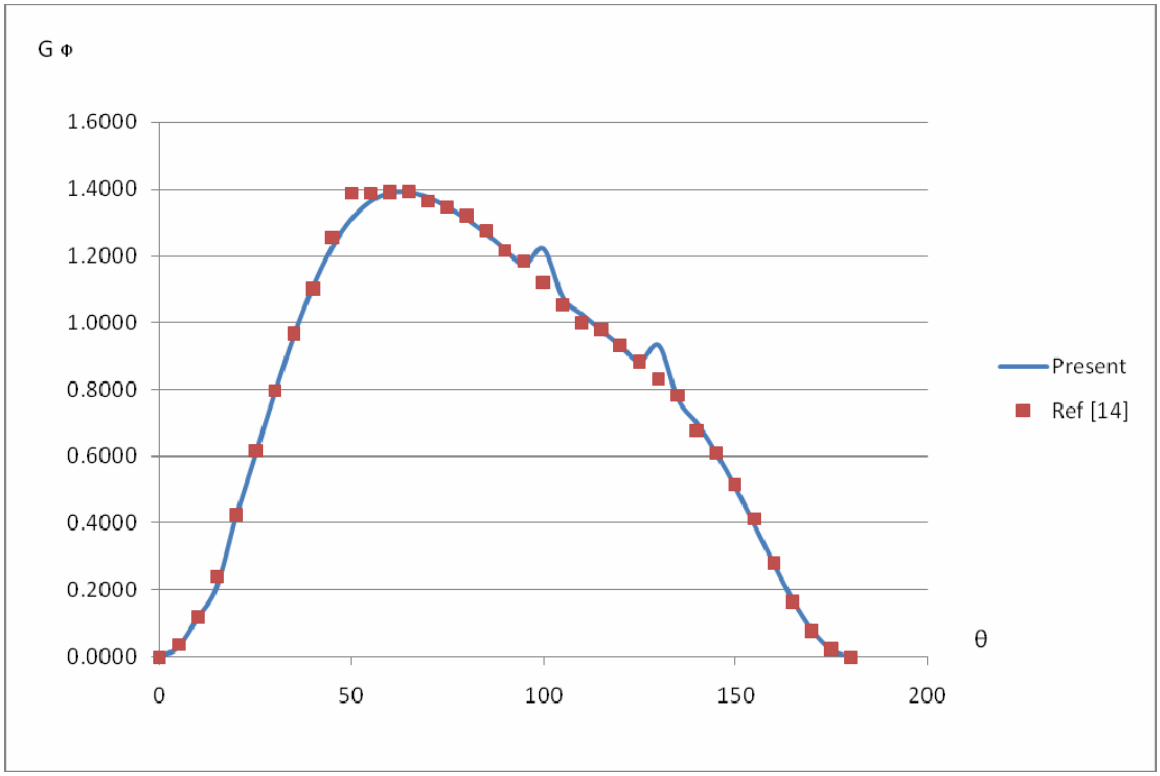

Figure (3.8): The normalized power gain G_ϕ as a function of ϕ

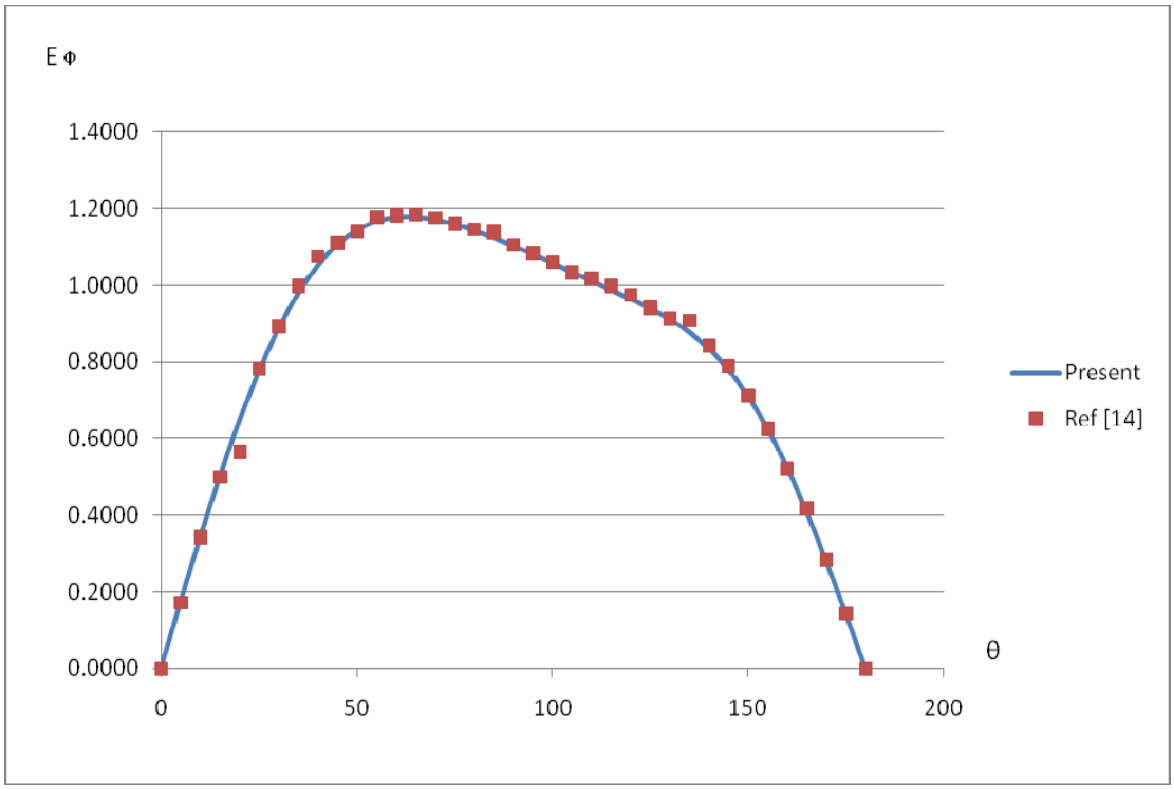

Figure (3.9): The normalized power gain E_ϕ as a function of ϕ

The Radar Cross Sections (RCS) $\left[\sigma / \lambda^2\right]$ can be seen in Table (3.6), and these data are compared with other results in figures (3.10), (3.11), (3.12) and (3.13).

Table 3.6: The Radar Cross Sections (RCS) $\left[\sigma / \lambda^2\right]$ with respect to the θ

θ	S_θ	$MAG\ S_\theta$	S_ϕ	$MAG\ S_\phi$
0	0.172	0.414	0.172	0.414
5	0.19	0.44	0.171	0.414
10	0.255	0.51	0.17	0.413
15	0.378	0.614	0.168	0.141
20	0.556	0.748	0.165	0.406
25	0.783	0.888	0.162	0.404
30	0.998	0.997	0.162	0.403
35	1.111	1.051	0.161	0.403
40	1.033	1.016	0.162	0.4
45	0.796	0.892	0.151	0.389
50	0.503	0.707	0.132	0.364
55	0.313	0.562	0.107	0.327
60	0.31	0.557	0.095	0.309
65	0.356	0.604	0.133	0.308
70	0.29	0.544	0.256	0.506
75	0.1	0.326	0.47	0.685
80	0.063	0.255	0.716	0.846
85	0.422	0.649	0.896	0.947
90	1.073	1.036	0.92	0.959
95	1.399	1.263	0.77	0.878
100	1.64	1.28	0.515	0.718
105	1.222	1.106	0.263	0.513
110	0.662	0.813	0.09	0.304
115	0.238	0.49	0.026	0.163
120	0.046	0.213	0.033	0.181
125	0.001	0.031	0.068	0.26
130	0.014	0.12	0.101	0.317
135	0.037	0.144	0.121	0.349
140	0.061	0.244	0.131	0.362
145	0.082	0.286	0.135	0.368
150	0.103	0.321	0.136	0.37
155	0.121	0.344	0.136	0.371
160	0.13	0.362	0.138	0.371
165	0.136	0.369	0.138	0.371
170	0.138	0.371	0.138	0.371
175	0.138	0.371	0.137	0.371
180	0.137	0.371	0.137	0.371

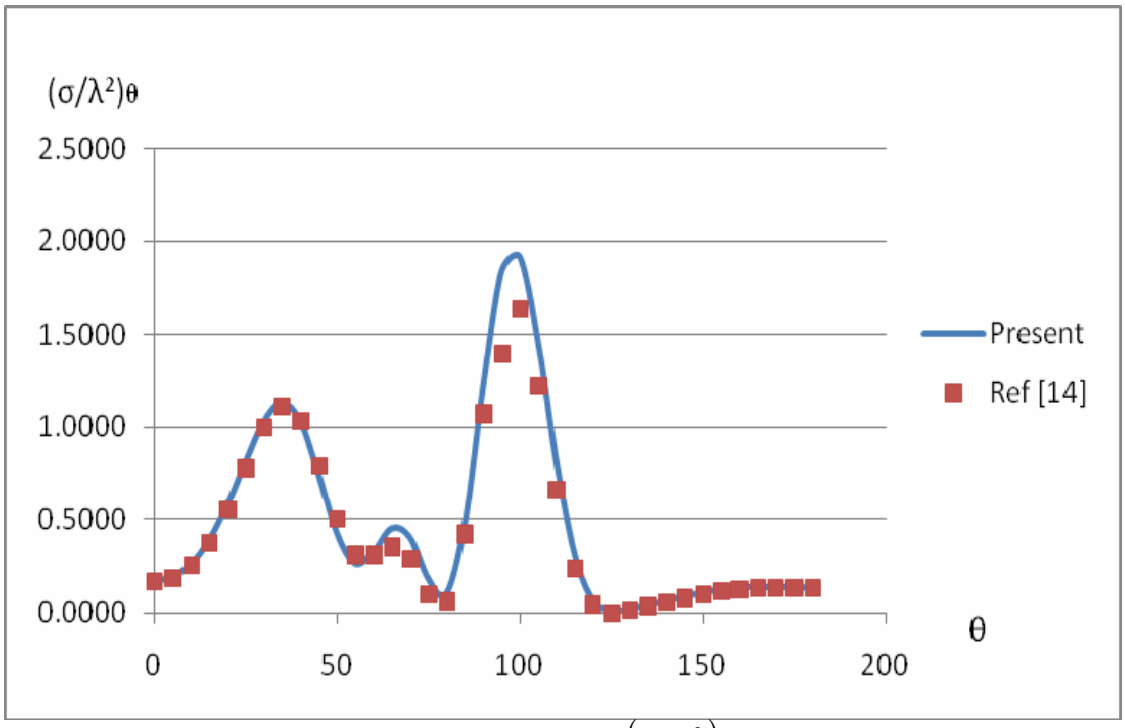

Figure (3.10): Radar Cross Sections $\left(\sigma / \lambda^2\right)_\theta$ as a function of θ

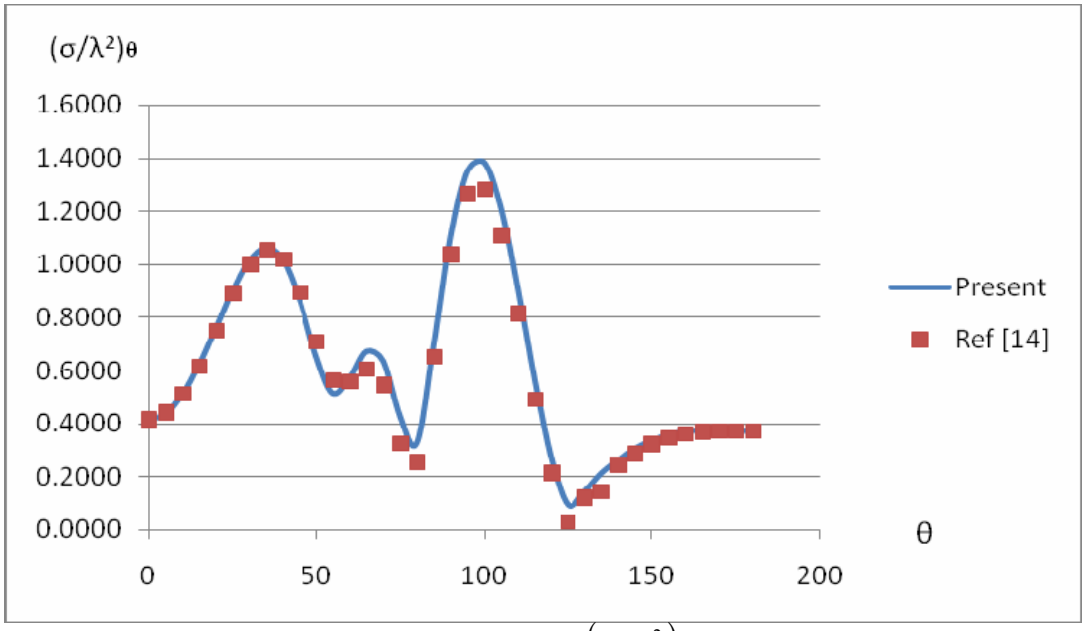

Figure (3.11): The magnitude of $\left(\sigma / \lambda^2\right)_\theta$ as a function of θ

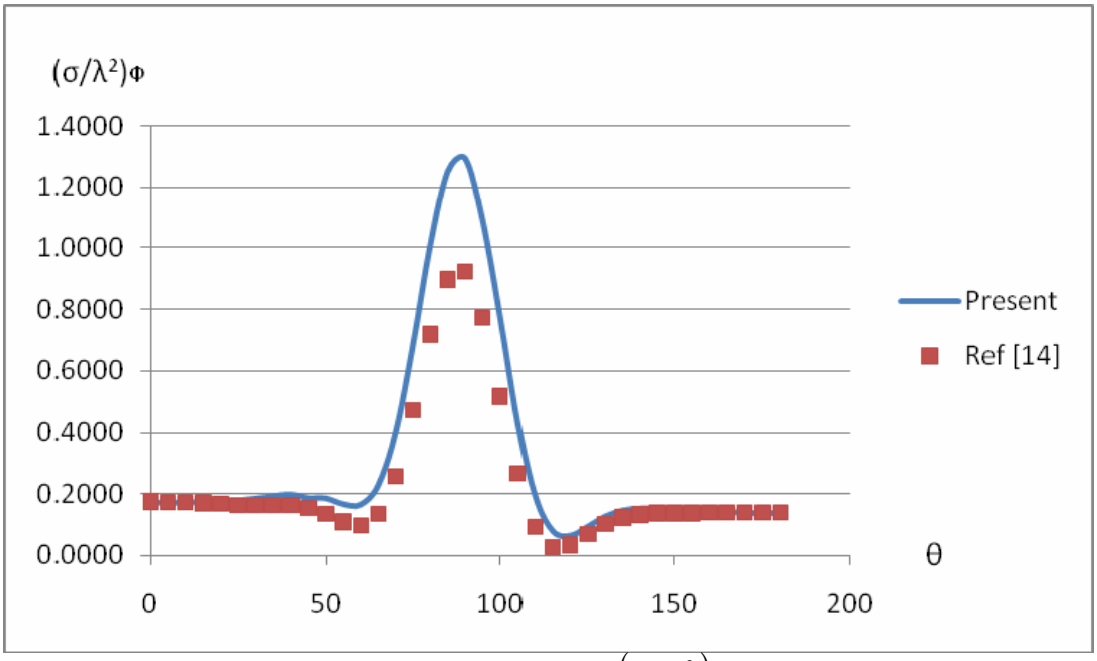

Figure (3.12): Radar Cross Sections $\left(\sigma / \lambda^2\right)_\phi$ as a function of θ

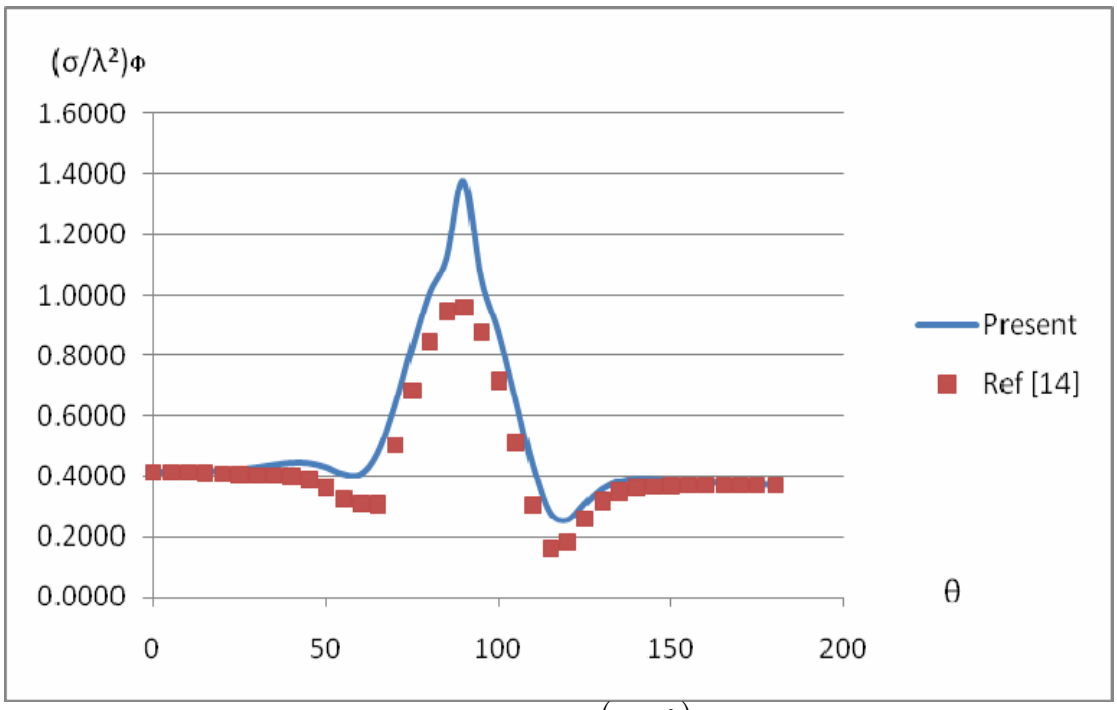

Figure (3.13): The magnitude of $\left(\sigma / \lambda^2\right)_\phi$ as a function of θ

In summary, the problems of electromagnetic scattering from finite bodies have been studied using two different approximations, the Method of Moment (MoM) where the electromagnetic scattering problem can be solved by reducing the operator equations to a system of linier equations written in a matrix form. Radar Cross Section (RCS) have been calculated and compared with other results. The far – field conditions are implicated in the Radar Cross Section definition. These results and all the programs can be well used in studying the scattering from dielectric or dielectrically coated materials. In this case, the induced surface currents are electric and magnetic currents.

APPENDIX

A.1 The mathematica work to solve the equations:

```
εr = 8.854*10^(-12)
k0 = 1/(4 Pi εr)
(*r = 1*)
μr = 1

m = 1
fm:=1 /  ( μr εr k0 k0 r r Sin[θ ]^2  - m^2)
(*fm = 1/fm1[r, θ];*)

a1 =(1/ fm^2) ( -I k0 εr r - I k0 r Cos[θ ] D[εr fm  Sin[θ ], θ ] - I
k0 Sin[θ ]^2  D[εr r r fm, r ] + I k0  εr r fm Sin[θ ]^2);

b1 =(1/ fm^2) ( -I k0 r Sin[θ ]^2  D[εr r*r fm, r ] - 2 I k0 εr r*r fm
Sin[θ ]^2 );

c1 = (1/ fm^2) ( -I k0 r Sin[θ ] D[εr fm Sin[θ ], θ ] - 2 I k0 εr r fm
Sin[θ ] Cos[θ ] );

d1 = (1/ fm^2) ( -I k0 εr r^3 fm Sin[θ ]^2);

e1 = (1/ fm^2) ( -I k0 εr r fm Sin[θ ]^2);

f1 = (1/ fm^2) ( I m Cos[θ ] D[ r fm , r ]- I m D[fm Sin[θ ], θ ]);

g1 = (1/ fm^2) ( - I m r Sin[θ ] D[fm, θ ]);

h1 = (1/ fm^2) ( I m r Sin[θ ] D[fm, r]);

a2 =(1/ fm^2) ( I k0 εr r + I k0 r Cos[θ ] D[μr fm Sin[θ ], θ ] + I k0
Sin[θ ]^2  D[μr r*r fm, r ] - I k0 μr r fm Sin[θ ]^2);

b2 =(1/ fm^2) ( I k0 r Sin[θ ]^2  D[μr r*r fm, r ] + 2 I k0 μr r*r fm
Sin[θ ]^2 );

c2= (1/ fm^2) ( I k0 r Sin[θ ] D[μr fm Sin[θ ], θ  ] + 2 I k0 μr r fm
Sin[θ ] Cos[θ ] );

d2 = (1/ fm^2) ( I k0 μr r^3 fm Sin[θ ]^2);

e2 = (1/ fm^2) ( I k0 μr r fm Sin[θ ]^2);

f2 = (1/ fm^2) ( I m Cos[θ ] D[ r fm, r ]- I m D[fm Sin[θ ], θ ]);

g2 = (1/ fm^2) ( - I m r Sin[θ ] D[fm, θ ]);

h2 = (1/ fm^2) ( I m r Sin[θ ] D[fm, r]);

a = 1/0.4
k = 16/a
ψ = Exp[-I k r]/r;

A1 = a1*ψ + b1 D[ψ,r] + d1  D[ψ,{r,2}];

B1 = b1*ψ + 2*d1 D[ψ,r];

C1 = c1*ψ;

D1 = d1*ψ;
```

```
E1 = e1*ψ;

F1 = f1*ψ + g1 D[ψ,r];

G1 = g1*ψ;

H1 = h1*ψ;

A2 = a2*ψ + b2 D[ψ,r] + d2 D[ψ,{r,2}];

B2 = b2*ψ + 2*d2 D[ψ,r];

C2 = c2*ψ;

D2 = d2*ψ;

E2 = e2*ψ;

F2 = f2*ψ + g2 D[ψ,r];

G2 = g2*ψ;

H2 = h2*ψ;

eq1 = A1 um[r ,θ] + B1 D[um[r ,θ],r] + C1 D[um[r ,θ],θ] + D1 D[um[r
,θ],{r,2}] + E1 D[um[r ,θ],{θ,2}] + F1 vm[r ,θ] + G1 D[vm[r ,θ],r] +
H1 D[vm[r ,θ],θ] □ 0;

eq2 = A2 vm[r ,θ] + B2 D[vm[r ,θ],r] + C2 D[vm[r ,θ],θ] + D2 D[vm[r
,θ],{r,2}] + E2 D[vm[r ,θ],{θ,2}] + F2 um[r ,θ] + G2 D[um[r ,θ],r] +
H2 D[um[r ,θ],θ] □ 0;


DSolve[{eq1,eq2},{vm[r,θ],um[r,θ]},{r ,θ}]
```

A.2 Spherical coordinates (r,θ,ϕ):

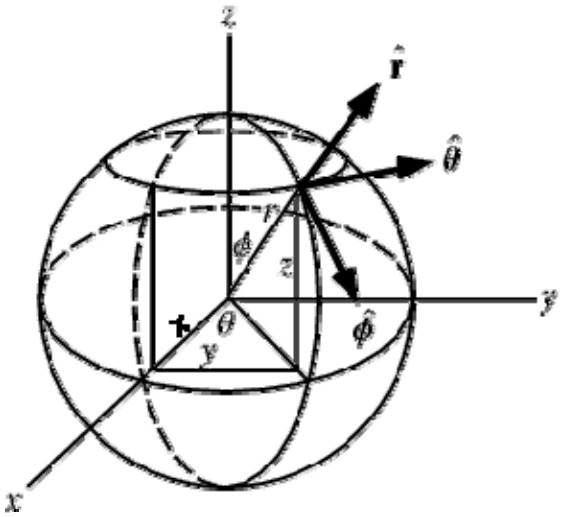

Fig (A.2.1): Spherical Coordinates.

$$\begin{aligned} x &= r\,\sin\theta\,\cos\phi \\ y &= r\,\sin\theta\,\sin\phi \\ z &= r\,\cos\theta \end{aligned} \qquad \text{A2.1}$$

$$\nabla\cdot E = \frac{1}{r^2}\frac{\partial}{\partial r}(r^2 E_r) + \frac{1}{r\sin(\theta)}\frac{\partial}{\partial\theta}(\sin(\theta)E_\theta) + \frac{1}{r\sin(\theta)}\frac{\partial}{\partial\phi}E_\phi \qquad \text{A2.2}$$

$$\begin{aligned} \nabla\times H = {} & \frac{1}{r^2\sin(\theta)}\left[\left(\frac{\partial}{\partial\theta}\left(r\sin(\theta)E_\phi\right)\right) - \frac{\partial}{\partial\phi}(rE_\theta)\right]\hat{r} \\ & + \frac{1}{r\sin\theta}\left(\frac{\partial}{\partial\phi}E_r - \frac{\partial}{\partial r}\left(r\sin(\theta)E_\phi\right)\right)\hat{\theta} + \frac{1}{r}\left(\frac{\partial}{\partial r}\left(rE_\theta\right) - \frac{\partial}{\partial\theta}E_r\right)\hat{\phi} \end{aligned} \qquad \text{A2.3}$$

A.3 Maxwell's equations:

Maxwell's equations represent one of the most elegant and concise ways to state the fundamentals of electricity and magnetism. From them one can develop most of the working relationships in the field. Because of their concise statement, they embody a high level of mathematical sophistication and are therefore not generally introduced in an introductory treatment of the subject, except perhaps as summary relationships.

Maxwell's equations can be written in terms of E and H as following:

$$\nabla \cdot E = \frac{\rho f}{\varepsilon}$$
$$\nabla \cdot H = 0$$
$$\nabla \times E = -\frac{\partial H}{\partial t} \qquad \text{A3.1}$$
$$\nabla \times H = \mu J f + \mu \varepsilon \frac{\partial E}{\partial t}$$

REFERENCES

References:

[1] Miller, E. K., "A Selective Survey of Computational Electromagnetic", IEEE Antenna and Propagation, pp. 1281-1305, 1988.

[2] V. Rodriquez-Pereyra, A. Z. Elsherbeni, and C. E. Smith, "A Body of Revolution Finite Difference Time Domain Method", Progress in Electromagnetic research, PIER 24, 257 – 277, 1999.

[3] Sebaq, A. M., "Studies on the Scattering of Steady State and Transient Electromagnetic Waves by Imperfectly Conducting and Coated Structures", A Ph.D. thesis, university of Manitoba, Canada, 1984.

[4] Raj Mittra, Richard K. G., "Radar Scattering from Bodies of Revolution using an Efficient Partial Differential Equation Algorithm", IEEE Antenna and Propagation, Vol. 37, No. 5, 1989.

[5] Mittra, R., Shuqing Li, Ji-Fu Ma, "Solving Large Body of Revolution (BOR) Problems using the Characteristics Basis Function Method and the FFT-Based Matrix Generation", IEEE Antennas and Propagation, pp. 3879-3882, 2006.

[6] Knott, E. E., Shaeffer, J. F. and Taley, M. J., "Radar Cross Section its Prediction, Measurements and Reduction", Artechhouse Inc., 1985.

[7] Edward, H. Newman, Ronald J, "Overview of MoM and UTD Methods at the Ohio State University", IEEE, pp.700-708, 1989.

[8] D. J. Brian and N. Williams, "Study of Modeling Methods for Large Reflector Antennas", 1996.

[9] Dybdal, R. B., "Radar Cross Section Measurments", IEEE, pp. 498-516 1987.

[10] Di Giampaolo, E. Bardati, F. "A method for multiple diffracted ray sampling in forward ray tracing", IEEE Antenna & Propagation, pp. 468-471, 2001.

[11] Mogus, A. A., "Scattering from Cylinders with Arbitary Surface Impedance", Proc. IEEE, pp. 812-817, Aug. 1965.

[12] Waterman, P. C., "Matrix Formulation of Electromagnetic Scattering", Proc. IEEE, pp. 805-811, Aug. 1965.

[13] Shuffer, J. F. And Louis, N. M., "Radiation from wire attached to bodies of revolution: Junction problem", IEEE Trans. Anten. & Propag. Vol. AP-29, No. 3, pp. 479-486, 1981.

[14] Mautz, J. R. And Harrington, R. F., "Radiation and Scattering from Bodies of Revolution". Appl. Sci. Res., Vol. 20, pp. 405-435, 1969.

[15] Hrrington, R. F. And Mautz, J. R., “Theory of characterstics modes for conduction bodies”, IEEE Trans. Anten. & Propag. Vol. AP-19, No. 5, p. 622-639, 1971.

[16] Kaki, A. N. M., “predication of radar cross section for some selected targets using method of moments”, A. M. E. Thesis submitted to the Univeristy of Technology, Baghdad, Iraq, 1994.

[17] Jedlicka, R. P., “Electromagnetic coupling into complex cavities through narrow slot aperture having depth and losses”, PhD. Dissertation submitted to the New Mexico state university, Mexico, 1995.

[18] Liu, D. R., “Simulation waves scattering from a randomly rough surface using wavelet expansion”, PhD. Dissertation submitted to the university of Texas at Arlington, USA, 1995.

[19] Sharpe, R. M., “Moment method analysis of complex structure containing cavity backed aperture”, PhD. Dissertation submitted to the university of Houston, USA, 1992.

[20] Khalbasi, K. I., “a DSP based multilevel iterative iterative technique for the moment method solution of large electromagnetic problems”, PhD. Dissertation submitted to the University of Kansas, USA, 1992.

[21] Al-Rizzo, H. M. Y., “Electromagnetic wave scattering from three dimensional coated and homogenous objects the GPMT and GMT; numerical modelling and applications (global positioning system)”, PhD. Dissertation submitted to the University of Brunswick, Canada, 1992.

[22] Crispin, T. W. JR and A. L. Maffatt, “Radar cross section estimation for simple shapes”, Proc. IEEE, No. 8, pp 833-848, Aug., 1965.

[23] Wu, T. K. And Leonard L. Tsai, “Scattering from arbitrarily shaped lossy dielectric bodies of revolution” Radio Sci., Vol. 12, No. 5, pp. 709-718, 1977.

[24] Pogorzelski, R. J., "On the numerical computations of scattering from inhomogeneous penetrable objects", IEEE Trans. Anten. & Propag. Vol. AP-26, No. 4, pp. 616-618, 1978.

[25] [38] Galisson, A. W. and Wilton, R. R., " Simple and efficient numerical methods for problems of electromagnetic radiation and scattering from surfaces", IEEE Trans. Anten. & propag., Vol. AP-28, No. 5, pr. 593-603, 1980.

[26] Philip L. H., Louis, N. M., and John, M. P. "Combined field integral equation formulation for scattering by dielectrically coated conducting", IEEE Trans. Anten. & propag., Vo1. AP-34, No. 4, pp. 510-520, 1986.

[27] Ga1isson, A. L., " An integral equation for electromagnetic from homogeneous dielectric bodies", IEEE Trans. Anten. & propag., Vol. AP- 32, No. 3, pp. 173-175,1984.

[28] Louis, N. M. and Putnam, J. M., '" Integral equation formulation for imperfectly conducting Scatterer", IEEE Trans. Anten. & propag., Vol. AP-33, No. 2, pp. 206-214, 1985.

[29] Harrington, R. F. Mautz, J. R., and Chang, Y., "Characteristics modes for dielectric and magnetic bodies", IEEE Trans. Anten. & propag., Vol. AP-2O, No. 2, pp. 194-198, 1972.

[30] Kishk, A. A. and Shafai, L. F., "The effect of various parameters of circular disk microstrip antennas on their radiation efficiency and the mode excitation", IEEE Trans. Anten. & propag., Vol. AP-34, No. 8, pp. 969- 976, 1986.

[31] James, JR, and Hall, P. S., “Handbook of microstrip antennas ", Chap. Two, Peter Peregrines, London, U. K., 1989.

[32] Pinhas, S., Shmuel S., and David T., "Moment method solution for centre feed microstrip disk antennas involving feed and edge current singularities'", IEEE Trans. Anten. & propag., Vol. AP-37, No. 12, pp. 1989.

[33] Kishk, A. A. and Shafai, L. F., "Numerical solution of scattering from coated bodies of revolution using different integral equation formulation", lE proc., Vol. 133 pt H., No. 3, pp. 227-232, 1986.

[34] Korada U., Allen T., and Sadasiva Mo Rao, "Electromagnetic scattering by arbitrary shaped three-dimensional homogenous dielectric objects", IEEE Trans. Anten & propag., Vol. AP-34, No~ 6, pp. 758-765, 1986.

[35] Wu, K. L., Delisle, G. Y., and Fang, D. G., "EM scattering of an arbitrary multiple dielectric coated conducting cylinder by coupled finite boundary element method", IEE proc., Vol. 137 pt. H., No. 1, pp.1-4, 1990.

[36] Delisle, G. Y., Fang, D. G., and Wu, K. L.,"Application of BEM to EM scattering by dielectric objects", Proc. Of Inter. Symp. On Anten. & EM theory, lnter. Academic publication pergoman press. 1st Edition, 1989.

[37] Xingchao, D. R. L., and Strohbehn, J. W., "Coupling of finite element objects", IEEE Trans. Anten. & propag., Vol. AP-38, No. 3, pp.386-393, 1990.

[38] Hassan, A. R., Shafai, L. F., and Michael H., "Plane wave scattering by a conducting elliptical cylinder coated by a non-confocal dielectric", IEEE Trans. Anten. & propag., Vol. AP-39, No. 2, pp.218-223, 1991.

[39] Schmitz, J. L., "Dual surface electric field integral equation for bodies of revolution in electromagnetic scattering", A. D. Eng. Dissertation submitted to the Univ. of Loweel. 1996.

[40] Harrington. R. F. and Mautz. J. R., "Control of radar scattering by reactive loading ", IEEE Trans. Anten. & propag., Vol. AP-20, No. 4, pp. 446-456, 1972.

[41] Mittra, R. and Gordan. R. K., "Radar scattering from bodies of revolution using an efficient partial differential equation algorithm ", IEEE Trans. Anten. & Propag. Vol. AP- 37, No. 5, pp. 538-545, 1989.

[42] Arvas. E. and Sarkar. T. K.., “RCS of two-dimensional structures consisting of both the dielectric and conductors of arbitrary cross section ", IEEE Trans. Anten. & Propag. Vol. AP. 37, No. 5, pp. 546-554, 1989.

[43] Wu, T. K., “Radar cross section of arbitrary shaped bodies of revolution ", Proc. IEEE. Vol. 77, No. 4, pp. 735-740, 1989.

[44] Abramowtiz, M. L. A. S., "Handbook of mathematical functions ", New York, Dover, 1970.

[45] Tsay, W. J., “Radiation and scattering from periodic geometries in inhomogeneous media ", PhD. Dissertation submitted to the university of Massachusetts, USA, 1995.

[46] Yoyssef, N. N., “Radar cross section of complex targets ", Proc. IEEE, Vol. 77, No. 5, pp. 722-734, 1989.

[47] Peters, T. H. and Volakis, J. L., “Application of conjugate gradient method FFT method to scattering from thin planar material plates ", IEEE Trans. Anten. & Propag. Vol. AP- 36, No. 4, pp.518-526, 1988.

[48] Sarkar, T. K. and Arvas, E., “Scattering cross section of composite conducting and lossy dielectric bodies” Proc. IEEE, Vol. 77, No. 5, pp. 788- 795, 1989.

[49] Catedra, M. F., Gaga, E., and Nuno, L., "A numerical scheme to obtain the RCS of three-dimensional bodies of resonant size using the conjugate gradient method and fast Fourier transform", IEEE Trans. Anten. & Propag. Vol. AP-37, No. 5, pp.528-537, 1989.

[50] Zwamhom, A. P. M. and Berg, P. M. V., "A week form of the conjugate gradient FFT method for plate problems ", IEEE Trans. Anten. & Propag. Vol. AP- 39, No. 2, pp.224-228, 1991.

[51] Tran, T. V. and Mcccomen, "An improved pulse-basis conjugate gradient FFT method for the thin conducting I2late problem ", IEEE Trans. Anten. & Propag. Vol. AP- 41, No. 2, pp.185-190, 1993.

[52] Ahuja, V., "Finite volume time domain method for Maxwell's equation on parallel computer (radar cross section)” PhD. Dissertation submitted to the Pennsylvania State University, USA, 1995.

[53] Casciato, M. D., "An electromagnetic code evaluation in the 100 to 1000 MHz region” A MSc. Dissertation submitted to the Florida Atlantic University, USA, 1995.

[54] Movahedi, A. J., "Electromagnetic radiation and scattering by a dielectric loaded conducting body coupled to an arbitrary wire ", PhD. Dissertation submitted to the university of Mississippi, USA, 1995.

[55] Penney, C. W., "Scattering from coated targets using a frequency domain surface impedance boundary condition in the finite difference time domain method (radar cross section)", PhD Dissertation submitted to the Pennsylvania State University, USA, 1995.

[56] Vinh, H., "Development of finite difference time domain solver for Maxwell's equations with application to radar signature prediction", PhD Dissertation submitted to the University of California, USA, 1994.

[57] Reuster, D. D., "Development of low RCS reflector antenna system", PhD Dissertation submitted to the University of Day ton, USA, 1994.

[58] Simons, N. R. S., "Development and application of differential equation numerical techniques to electromagnetic scattering and radiation prob1ems", PhD Dissertation submitted to the Manitoba University, Canada, 1994.

[59] Groenewald, J. J., "Synthesis of radar cross section using antenna array", A M. E. Eng. Dissertation submitted to the University of Pretoria, South Africa, Africa, 1994.

[60] A1kanhal, M. A.," E1ectromagnetic scattering from chairal cylinders of arbitrary cross section", PhD. Dissertation submitted to the Syracuse University, USA, 1994.

[61] Kolbehdari, M. A., "Numerical analysis of electromagnetic field from a class of composite cylinders", PhD. Dissertation submitted to the Temple university, USA, 1995.

[62] Antilla, G. E., "Radiation and scattering from complex three dimensional geometries using s hybrid finite element integral equation approach", PhD. Dissertation submitted to the university of California at Loss Anglos, USA, 1993.

[63] Uslenghi, P. L. E., "Electromagnetic scattering" Academic Press Inc., New York, USA, 1978.

[64] P. Jacobsson and T. Rylander, RVK08 conference, June 9-13, 2008, Vaxjö, Sweden.

[65] M. Cheney and B. Borden, Imaging moving targets from scattered waves, Inverse problems 24 (2008) 035005.

[66] Anyong Qing, "Electromagnetic Imaging of two Dimensional Perfectly Conducting Cylinders with Transverse Electric Field" IEEE, vol.50, No.12, (2002) 1786.

[67] F.J.Villegas, Y.H.Sammi, D.R.Jackson, "A Hybrid MoM Solution of Scattering from Finite Arrays of Cylindrical Cavities in a Ground Plane" IEEE, vol.51, No.9, (2003) 2369.

[68] C.L.Rino, K.J.Doniger and J.R.Martinez "The Method of Ordered Multiple Interactions for Closed Bodies" IEEE, vol.51, No.9, (2003) 2327.